

Sprayable Hydrogel Sealant for Gastrointestinal Wound Shielding

Gonzalo Muñoz Taboada, Daniel Dahis, Pere Dosta, Elazer Edelman, and Natalie Artzi*

Naturally occurring internal bleeding, such as in stomach ulcers, and complications following interventions, such as polyp resection post-colonoscopy, may result in delayed (5–7 days) post-operative adverse events—such as bleeding, intestinal wall perforation, and leakage. Current solutions for controlling intra- and post-procedural complications are limited in effectiveness. Hemostatic powders only provide a temporary solution due to their short-term adhesion to GI mucosal tissues (less than 48 h). In this study, a sprayable adhesive hydrogel for facile application and sustained adhesion to GI lesions is developed using clinically available endoscopes. Upon spraying, the biomaterial (based on polyethyleneimine-modified Pluronic micelles precursor and oxidized dextran) instantly gels upon contact with the tissue, forming an adhesive shield. In vitro and in vivo studies in guinea pigs, rabbits, and pig models confirm the safety and efficacy of this biomaterial in colonic and acidic stomach lesions. The authors' findings highlight that this family of hydrogels ensures prolonged tissue protection (3–7 days), facilitates wound healing, and minimizes the risk of delayed complications. Overall, this technology offers a readily adoptable approach for gastrointestinal wound management.

invasive techniques, such as endoscopic mucosal resection (EMR) and endoscopic submucosal dissection (ESD),^[9] are commonly used during GI screening. EMR utilizes an endoscopic snare to resect early-stage or pre-cancerous superficial polyps; while ESD carefully removes lesions by resecting the mucosal and submucosal layers.^[10] These procedures reduce the incidence of colorectal cancer^[3,11] but are not without complications.

Over 15 million colonoscopies are performed annually in the US alone.^[12] Although EMR and ESD are considered to be safe, the increase in the number of screening procedures results in a large number of serious adverse events such as bleeding, intestinal wall perforation, and lesion infection.^[13,14] The most common adverse event is delayed bleeding and its occurrence is dictated by multiple factors such as the size and location of the excised polyp, resection technique, and other comorbidities.^[15–17]

Bleeding can occur after patient discharge, making complications harder to detect and treat in time,^[15,18] leading to severe blood loss and potential need for blood transfusion. When intestinal wall perforation ensues, emergency surgery and prolonged hospitalization are required.^[19–21] In addition, bleeding can result from GI ulcers.^[22]

The current solution for controlling intra- and post-procedural bleeding is wound closure using five to ten metallic clips^[23]

1. Introduction

Gastrointestinal (GI) tract malignancies are a significant global health burden, accounting for 26% of all cancer cases and one-third of cancer-related deaths.^[1,2] Screening technologies such as GI endoscopy and other non-invasive procedures have played a critical role in detecting early-stage tumors over the last few decades.^[3–8] Minimally

G. Muñoz Taboada, D. Dahis
BioDevek
Boston, MA 02134, USA
G. Muñoz Taboada
Institut Químic de Sarrià
Universitat Ramon Llull
Barcelona 08017, Spain

P. Dosta, E. Edelman, N. Artzi
Brigham and Women's Hospital
Harvard Medical School
Boston, MA 02115, USA
E-mail: nartzi@bwh.harvard.edu

P. Dosta, E. Edelman, N. Artzi
Institute for Medical Engineering and Science
Massachusetts Institute of Technology
Cambridge, MA 02139, USA

P. Dosta, N. Artzi
Wyss Institute for Biologically-Inspired Engineering
Harvard University
Boston, MA 02115, USA

N. Artzi
Broad Institute of Harvard and MIT
Cambridge, MA 02139, USA

The ORCID identification number(s) for the author(s) of this article can be found under <https://doi.org/10.1002/adma.202311798>

© 2024 The Authors. Advanced Materials published by Wiley-VCH GmbH. This is an open access article under the terms of the [Creative Commons Attribution-NonCommercial-NoDerivs](#) License, which permits use and distribution in any medium, provided the original work is properly cited, the use is non-commercial and no modifications or adaptations are made.

DOI: 10.1002/adma.202311798

that are challenging to apply, expensive, time-consuming, and rarely prevent post-operative bleeding.^[24–26] Their size allows introduction via the endoscope channel (<3 mm in diameter), but that means that they can only approximate tissues that are less than 20 mm apart, leaving high-risk large lesions unprotected.^[24] Hydrogel-based technologies have been proposed to facilitate the safe closure of wounds^[27–30] due to their biocompatibility, biodegradability, and ability to be tuned to exhibit adequate mechanical properties. In fact, several bioadhesive technologies have been commercialized for numerous indications,^[31,32] including BioGlue, Coseal, and Tisseel which have been FDA approved for vascular purposes, Duraseal and Adherus for dura sealing, and Progel for lung sealing.

Yet, hydrogel-based solutions proposed for luminal GI application broadly achieve less than 48 h of mucosal adhesion,^[17,33–37] and the best options are limited to hemostatic powders that gel upon contact with actively bleeding wounds.^[17] While powders work fairly well for acute hemostasis, they were not designed to provide prolonged protection of the lacerated area, do not homogeneously cover the target lesion, and lack mucosal adhesion as observed by their short residence time (few hours to 42 hours following application).^[17,38] Further, these solutions are limited to actively bleeding lesions only and suffer from the high risk of nozzle clogging upon contact with the GI.^[39]

Due to these shortcomings, no commercially available sealant is able to effectively prevent post-operative and delayed GI complications (3–7 days post the procedure). The lack of mucosal sealants in the market can be attributed to the challenge of engineering materials that are biocompatible and afford sustained adhesion to mucosal tissues where peristalsis forces and the passing of GI content may delaminate the sealant,^[17] in addition to withstanding exposure to acidic fluids. However, it also must be sufficiently soft and compliant to match with that of the tissue to prevent strictures or luminal occlusion. Upon application, the material must remain at the site, even when applied against gravity, and adhesion should be titrated to the tissue while preventing unintended adhesion to the opposite intestinal wall, which could lead to luminal occlusion.^[40] A material that fulfills these design criteria would, in principle, enable the natural wound healing process to occur. For clinical adoption, its delivery must be compatible with the existing colonoscopy equipment and not extend the procedure time significantly (ideally < 10 min).

With the goal to fulfill the necessary requirements for endoscopic luminal GI sealing and surmounting the limitations of current technologies, we designed a sprayable sealant based on polyethyleneimine (PEI)-modified Pluronic precursor and oxidized dextran. It is well-documented that multibranched or dendritic high molecular weight polymers outperform their linear counterparts in achieving high adhesion and adequate mechanical properties when used as crosslinking agents to form hydrogel networks.^[41–43] Yet, their association with cytotoxic effects,^[44] issues with stability in solution, and brittleness of the hydrogel network due to its rigid structure^[45] compromise their suitability for endoscopic applications. To circumvent these drawbacks, we synthesized an amine-modified block-copolymer (Pluronic) that self-assembles into micelles in aqueous solutions (PluPEI).^[46,47] Each Pluronic chain was end-capped with \approx six primary amine groups on each side. However, in its micellized form, the surface of each micelle displayed hundreds of amine groups, primed for

instantaneous covalent cross-linking. This strategy, akin to the formation of dendritic structures, offers several advantages. As the hydrogel network forms, the Pluronic creates high-density amine cores, but when degrading over time, only individual PluPEI molecules are released, mitigating potential toxicity concerns associated with highly protonated amine dendrimers. Further, the micelle structure, held together by reversible hydrophobic interactions, can yield under stress, dissipating energy without compromising the integrity of the hydrogel network.^[48] Moreover, in addition to the covalent interactions between aldehyde groups and tissue provided by oxidized dextran, the high density of the amine groups exposed in micelles promotes robust and sustained adhesion to biological tissue through ionic interactions between oppositely charged groups and other electrostatic interactions such as hydrogen bonds promoted by the micellar conformation and high amine density of the PluPEI. This amalgamation of unique attributes paves the way for the PluPEI material family as a versatile and robust tool for mucosal adhesion.

Following these design principles, we put forth GastroShield, a novel class of sprayable bio-adhesive hydrogel intended for applications in gastrointestinal (GI) tissues. This unique material is formulated by dispensing two low-viscosity precursors—oxidized dextran and PluPEI—that swiftly react upon contact with mucosal tissue to form a cohesive tissue shield. The reduced viscosity of the precursors enables their facile delivery through a catheter inserted into an endoscope channel. Concurrently, the rapid gelation time, facilitated by the high amine concentration on the micelle surface, ensures the material's localization to the target area; thus, minimizing risks of off-target adhesion and dripping. This study demonstrates that GastroShield provides substantial protection to GI wounds and lacerations against the adverse conditions of gastric juices; while, maintaining high biocompatibility, adhesive strength, and material integrity. Importantly, this material supports protection of the affected area for several days following application, thereby enabling the body's natural healing mechanism to ensue. The findings presented in this study highlight the potential of GastroShield to address the currently unmet clinical needs for effective wound management in the highly dynamic environment of the GI tract.

2. Results

2.1. Design and Characterization of Submucosal Adhesive Hydrogel

Intestinal or gastric bleeding can arise naturally, as in the case of ulcers, or from lesions created following interventional procedures such as polyp or tumor removal (**Figure 1a**). The current solution for controlling intra- and post-procedural GI bleeding is wound closure using metallic clips, which are costly, require application by skilled personnel, fall off prematurely, and have limited efficacy in preventing post-operative bleeding.^[24–26] Recent innovations in the field were introduced by the development of hemostatic technologies to facilitate safe bleeding control of wounds.^[27–30] Hemostatic powders such as Endoclot, Hemospray, and Nexpowder,^[17] can be used to control acute bleeding during endoscopic procedures. However, they lack mucosal adhesion properties and are therefore washed away within hours following application, can be applied only to actively bleeding

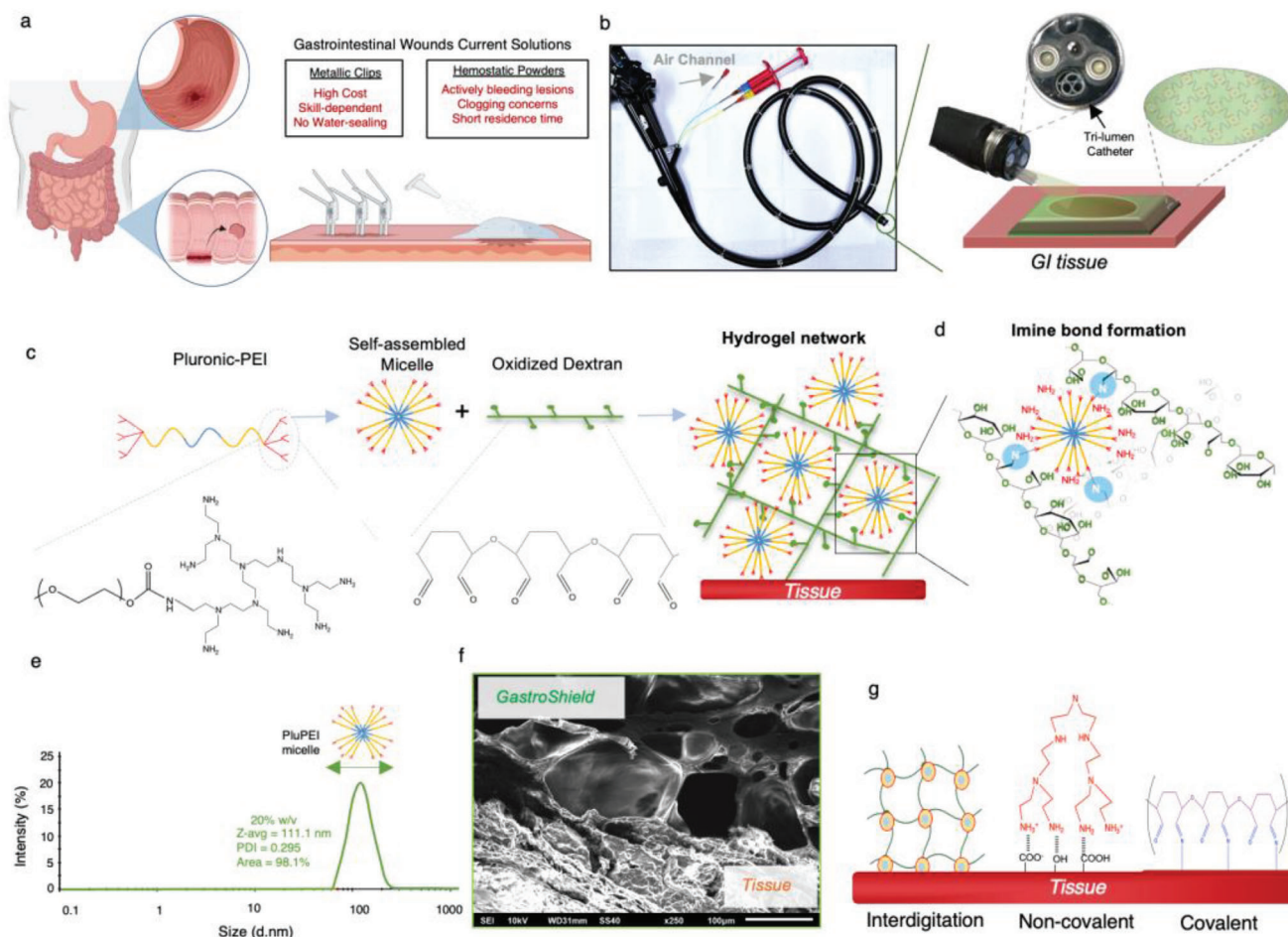


Figure 1. GastroShield uses, composition, and interactions with the tissue. a) Existing technologies fail to enable prolonged GI wound protection and are hard to apply. b) GastroShield is designed for facile endoscopic application to the mucosal tissue using a tri-lumen catheter. c) PEI-functionalized pluronic self-assembled micelles interact with oxidized to form the polymeric network. d) Imine bonds are created between amine groups of the PluPEI and aldehydes in oxidized dextran. e) Dynamic light scattering of a solution of 20% w/v of PluPEI at 25 °C. f) A SEM image showing the structure of the hydrogel attached to intestinal tissue. g) GastroShield hydrogel network interacts with the tissue via interdigitation, ionic and electrostatic interactions, and covalent imine bonds.

lesions, and have a high risk of nozzle clogging due to the moisture in the GI environment.^[17,38] These aspects compromise their efficacy in decreasing delayed bleeding and wide adoption.

GastroShield is designed to quickly form a tissue shielding barrier upon mixing the two solutions (PluPEI and oxidized dextran). It is delivered using a millimetric tri-lumen catheter (overall diameter of < 3.2 mm) that can be inserted into any commercial endoscope working channel. When sprayed, it creates a thin and strong hydrogel coating over the lesion (Figure 1b). This is achieved by crosslinking the oxidized dextran component (in one of the catheter lumens) with PEI modified Pluronic self-assembled micelles (in the other lumen) (Figure 1c) via imine bond formation between amines and aldehydes upon mixing (Figure 1d). The use of PluPEI micelles (Figure 1e) as crosslinkers provides to the hydrogel matrix superior properties due to its capacity to dissipate energy under stress.^[48,49]

The components of the hydrogel are sprayed in a liquid form, allowing them to interdigitate into the tissue (Figure 1f). Upon mixing, the polymers interact internally to form the hydrogel ma-

trix via imine chemistry, and externally, with the tissue by forming analogous bonds with tissue amines. These bonds are stable and reversible, allowing for robust adhesion, reversibility, and gradual hydrolytic material degradation into biocompatible precursors over time. Further, additional non-covalent interactions between the gel and tissue increase its adhesion, including interdigitation with the tissue surface upon application, ionic interactions between oppositely charged groups, and other electrostatic interactions such as hydrogen bonds promoted by the micellar conformation and high amine density of the PluPEI (Figure 1g).

We initially investigated various formulations to fulfill the requirements for GI application—ultrafast gelation time, low viscosity for long catheter compatibility, low swelling, long stability, and low friction coefficient of the material platform (Figure 2a)—ultimately identifying a family of formulations that fulfill all of these requirements (Figure 2b).

To achieve the required, near-instant gelation, we sought to end-cap the Pluronic molecule with an amine-containing molecule. Using a single or dual amine modification on each

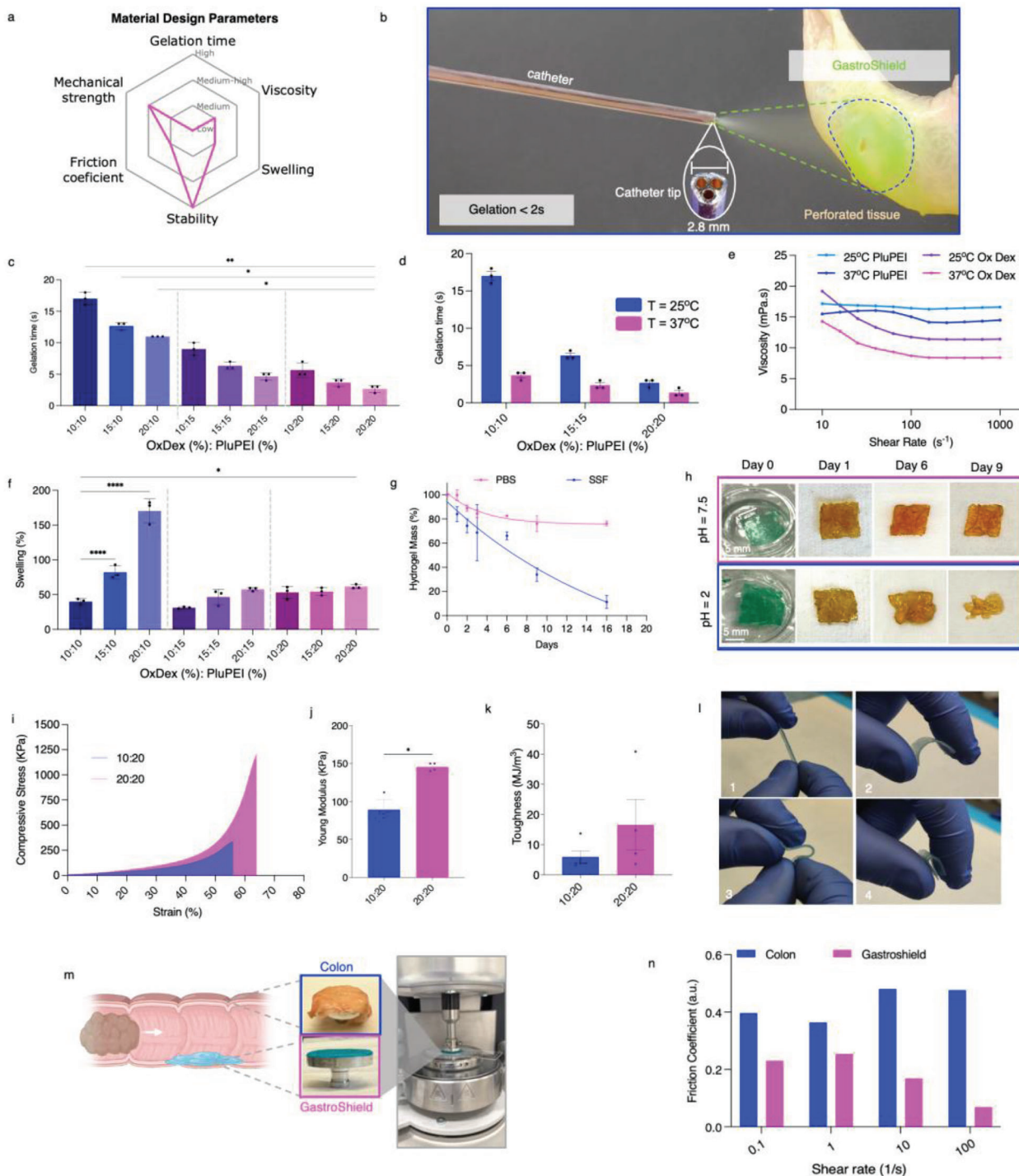


Figure 2. Mechanical characterization of the sealant. a) GastroShield is designed to achieve the desired target product profile of a luminal gastrointestinal sealant. b) GastroShield application via a catheter onto a perforated colon ex vivo. The fast gelation time enables dripless delivery onto vertical surfaces. The 2.8 mm total catheter diameter enables its compatibility with all commercially available endoscope channels. c) Gelation time of multiple formulations of the GastroShield material platform, $n = 3$ samples per group. d) Gelation time of GastroShield formulations at room temperature and 37 °C, $n = 3$ samples per group. e) Viscosity of the individual GastroShield polymer components at different shear rates at a concentration of 200 mg mL⁻¹. f) GastroShield Swelling at 24 h, $n = 3$ samples per group. g) Degradation of the hydrogels over 16 days incubated at 37 °C in PBS and simulated stomach fluid (SSF), $n = 3$ samples per group. h) Representative images of GastroShield samples over time. i) Compressive Stress–Strain curves. j) Young's Modulus, $n = 5$, 4 samples per group for the 10:10 and 20:20 sealants, respectively. k) Toughness of lead GastroShield formulations, $n = 5$, 4 samples from left to right. l) GastroShield hydrogel displays the flexibility required in many GI indications. m) Scheme of lubrication test performed comparing the naïve colon versus GastroShield to enable facile transit of GI content. n) Measured friction coefficient at $F = 2$ N. Data are expressed as mean \pm SEM; * $p < 0.05$, ** $p < 0.01$, *** $p < 0.001$, and **** $p < 0.0001$.

side of the polymeric chain did not result in fast-gelling materials. However, when using low molecular weight polyethyleneimine, near instant gelation times were achieved. The resulting Pluronic contained ≈ 12 primary amine groups per chain (Figure S1a,b, Supporting Information). Dextran was 50% oxidized using sodium meta-periodate as previously described.^[27,42] The successful modification was confirmed via NMR and FTIR (Figure S1c,d, Supporting Information).

When studying hydrogels formed with the two polymers, we found that gelation time inversely correlates with polymer concentration. Increasing the solid content of either of the components accelerates the reaction rate and therefore reduces the gelation time. Doubling the concentration, from 10% oxidized dextran and 10%-PluPEI to 20% of each component, decreases the gelation time from 17 to less than 4 s. Quick gelation becomes critical to prevent material dripping from the target area. The PluPEI component seems to have a larger effect on controlling gelation time compared with the dextran (Figure 2c). When tested at a physiological temperature (37 °C), the high-concentration formulations achieved near-instantaneous gelation times of < 2 s (Figure 2d).

In contrast, the viscosity of GastroShield components at their highest concentration (200 mg mL⁻¹) did not significantly increase when tested at 25 °C and 37 °C (Figure 2e). Under both conditions, the viscosity remained lower than 20 mPa·s across a wide range of shear rates. This low viscosity is crucial for ensuring proper flow through the thin catheters used in endoscopy (≈ 1 mm ID) and for maintaining an adequate spraying pattern.

When studying swelling, we observed that this element was primarily influenced by PluPEI concentration (inversely proportional) and the PluPEI:Oxidized Dextran ratio (Figure 2f). Formulations containing 15% and 20% PluPEI exhibited swelling values of $\approx 50\%$ at 24 h. While hydrogel swelling has been reported to enhance biocompatibility, excessive swelling must be carefully considered as it may lead to lumen obstruction^[50,51] or loss of mechanical and adhesive properties.^[52] To assess this, we further characterized the maximum lateral (x) and height (z) swelling of hydrogels, observing a lateral average swelling of $14.3 \pm 0.9\%$ and $30 \pm 6.2\%$, and height average swelling of $13.3 \pm 4.1\%$ and $24.3 \pm 9.6\%$ for formulations 10:20 and 20:20 (Oxidized Dextran(%):PluPEI(%), respectively (Figure S2a, Supporting Information). The lower GI lumen has a diameter ranging from 3 to 8 cm^[53] and the narrower section of the stomach of ≈ 3.3 cm.^[54] In the swollen state, GastroShield is designed to display a maximal thickness of ≈ 2 mm, eliminating concerns regarding lumen occlusion.

To evaluate the stability of GastroShield under various GI conditions, we monitored its degradation at pH 7 (simulating intestinal conditions) and at pH 2 (simulating stomach conditions) (Figure 2g). Imine bonds are less stable in acidic environments, where hydrolytic degradation dominates. Nevertheless, GastroShield formulations retained over 50% of their initial solid content after 1 week, when incubated in a large excess of highly acidic buffer (pH = 2) which was renewed daily (Figure 2h), confirming their ability to protect lesions in the stomach for an extended period of time. Importantly, we observed a stable $\approx 80\%$ of water-content in the materials incubated at both conditions over time, meaning that no significant swelling or change of polymer:water ratio occurred in this period (Figure S2b, Supporting

Information). On day 16, hydrogels that were incubated at pH 7 retained more than 80% of their initial solid content.

We next investigated the compressive strength of GastroShield (Figure 2i; Figure S2c, Supporting Information) and confirmed that increasing gel solid content increases the maximum strain at fracture (57% and 63% for the 10:20 and 20:20 formulations, respectively, Figure S2d, Supporting Information), as well as the stress at fracture (677 and 1646 KPa, for the 10:20 and 20:20 hydrogels, respectively, Figure S2e, Supporting Information). This effect was also seen in the measured Young's modulus (89.2 KPa vs 145.5 KPa) (Figure 2j) and toughness (5.97 vs 16.59 MJ m⁻³) for the 10:20 gels and 20:20, respectively (Figure 2k). We confirmed the flexibility of the gels manually via intense bending (Figure 2l).

To assess the sprayability of GastroShield polymeric solutions via millimetric endoscopic catheter at physiological temperature, viscosity, and storage and loss moduli were assessed at 25 °C and 37 °C. The high ratio between loss modulus (G'') and storage modulus (G') at a broad range of frequencies (1–100 Rad s⁻¹) and temperatures (25 °C and 37 °C) confirms the sprayability of both components (Figures S2f and S2g, Supporting Information, respectively). We also tested the tensile adhesion strength of these hydrogels, measuring 10.4 and 10.1 KPa for the 10:20 and 20:20 formulations (%Oxidized Dextran: %PluPEI) (Figure S2h, Supporting Information).

To confirm the superior mechanical properties conferred by PluPEI micelles, we compared GastroShield to an identical hydrogel formulation containing the same concentration of amines using PAMAM-dendrimers as crosslinkers instead of PluPEI (Figure S3, Supporting Information). We observed that while the gelation time of PAMAM-dendrimer hydrogels was 6.75 ± 0.25 s, PluPEI-hydrogels exhibited a gelation time of < 2 s. In addition, we tested the mechanical properties of both hydrogels under compression. We found that dendrimer-based hydrogels exhibited on average, maximal compressive strain at fracture of $24.6 \pm 2.8\%$; while, PluPEI hydrogels depicted $54.5 \pm 6.3\%$, an increase of $\approx 120\%$.

In addition to high adhesion and instantaneous gelation, the material must allow for easy transit of solid materials in the GI tract by minimizing resistance (shear stress) to their passage. To investigate this, we examined the friction coefficient (FCO) of a thin coating of GastroShield across multiple shear rates and compared it to naïve colon tissue (Figure 2m). GastroShield depicted lower COF values than the tissue for all studied shear rates, exhibiting ratios of $\text{FCO}_{\text{GastroShield}} / \text{FCO}_{\text{Colon}}$ of 0.58, 0.7, 0.35, and 0.15 for the shear rates of 0.1, 1, 10, and 100 s⁻¹, respectively (Figure 2n).

Taken together, these results demonstrate the versatility of this family of sealants as a function of formulation that can achieve instantaneous gelation, minimal swelling, and in vitro durability for at least 14 days in physiological pH and at least for 7 days in acidic pH, underscoring its stability potential for days/weeks following GI lesion application. Further, the sealant depicts high compressive strain and high compressive load at fracture, validating its ability to resist the pressures of the GI tract; while, facilitating the passage of contents across its lumen due to its lower friction coefficient in comparison to the colonic tissue. Lastly, the precursor solutions depict a shear thinning effect at higher shear rates, enabling facile spraying characteristics.

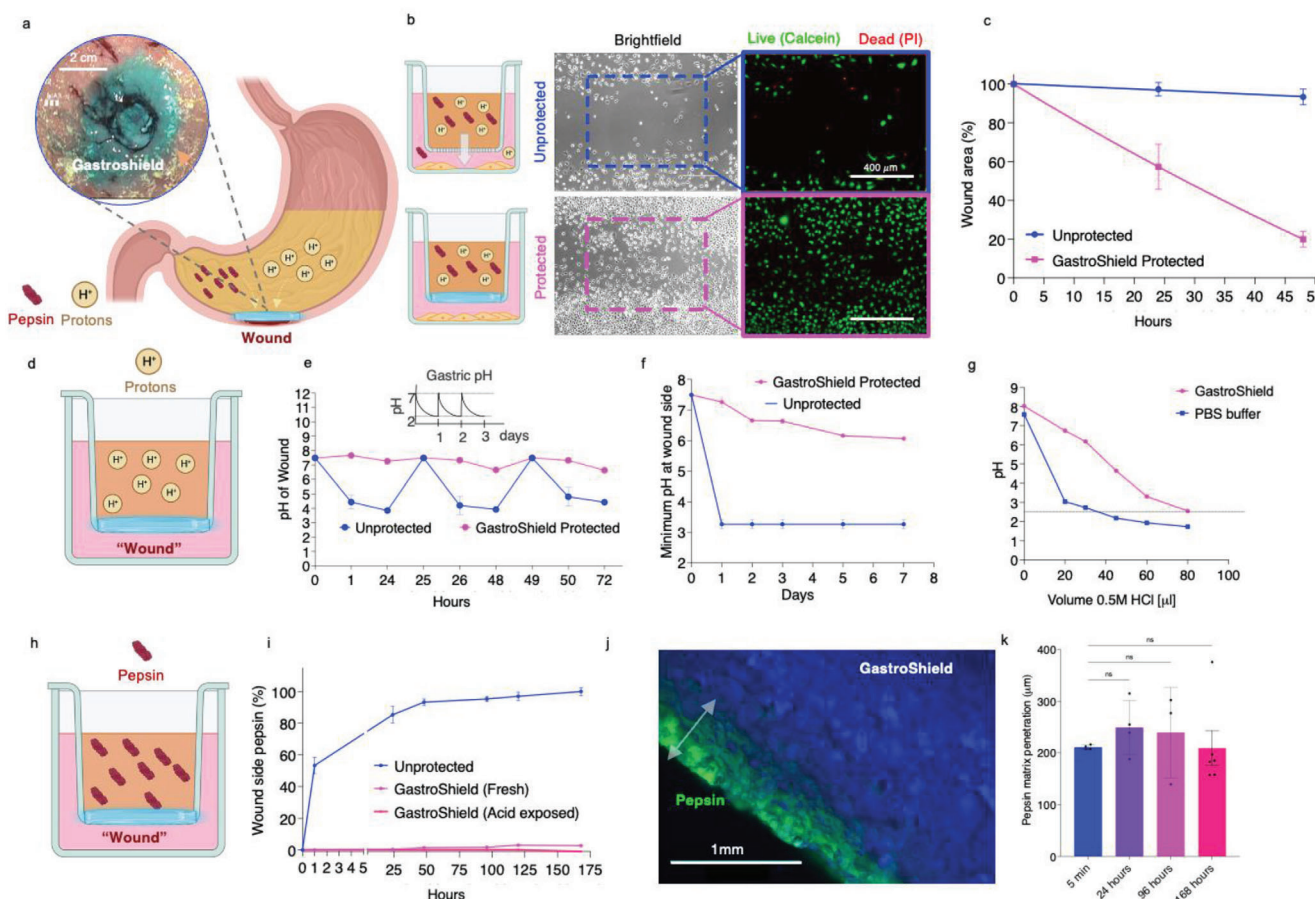


Figure 3. Sealant-mediated wound shielding in the presence of enzymes and in an acidic environment. a) Schematic representation of a wound ulcer protected from acid and enzymatic juices by GastroShield. Scale bar = 2 cm. b) Wound healing scratch model with GastroShield protecting a monolayer of L929 cells from low pH and 1.8 mg mL^{-1} of pepsin. Live/dead staining confirms that the delay in growth is not a result of massive cell death but rather due to delayed scratch closure. Images were collected 48 h following initiation of the scratch assay. c) Quantification of the remaining wound area in the GastroShield protected and unprotected groups, $n = 3$ samples per group per time point. d) In vitro setup to mimic GastroShield wound protection from acidic environment. e) pH recorded in the “wound side” (bottom transwell) that was either unprotected or protected with GastroShield, $n = 3$ samples per group per time point. f) Minimum pH recorded in the “wound side” of the transwell over 1 week with daily addition of fresh SSF to the top chamber and PBS in the wound side, $n = 2$, and 3 samples/timepoint for unprotected and GastroShield protected groups, respectively. g) Buffering capacity of GastroShield compared to PBS. The PEI component of the hydrogel acts as a proton sponge, neutralizing acid. h) In vitro setup to mimic GastroShield wound protection from lytic enzymes. i) Quantification of the pepsin concentration in the wound side for unprotected transwell, fresh GastroShield, and GastroShield transwell that had been incubated in SSF over 7 days. $n = 3$ samples per group. j) Representative images of fluorescently labeled pepsin that is retained on the surface of GastroShield hydrogel. k) Pepsin penetration into the GastroShield matrix is limited and plateaus at $200 \mu\text{m}$ after 24 h without further penetration, $n = 4, 4, 3$, and 6 fluorescence profiles analyzed from left to right. Data are expressed as mean \pm SEM; * $p < 0.05$, ** $p < 0.01$, *** $p < 0.001$, **** $p < 0.0001$.

2.2. Wound Protection

The acidic environment of the stomach can hinder the healing process of lesions or ulcers.^[55] Stomach ulcers are devoid of their protective mucosal layer and are therefore exposed to acidic conditions or catabolic agents that are activated at low pH, including pepsin and other digestive enzymes. In fact, activated pepsin degrades regenerative agents that promote neovascularization and healing.^[55,56] We therefore conducted a series of experiments that investigated GastroShield’s ability to protect the tissue from the acidic environment and the presence of enzymes (Figure 3a).

We used a wound scratch assay to quantify the rate of cell migration following an induced scratch in the well, which is driven by secreted growth factors from cells at the wound margin.^[39]

We used a transwell setup (Figure 3b) in which the top chamber containing an acidic solution (pH = 2) with pepsin (1.8 mg mL^{-1}) was separated from cells (L929) in the bottom chamber by a layer of GastroShield. In the untreated group (without GastroShield), the cells displayed a delay in wound healing compared to the protected group. Unprotected cells repopulated only $6.7 \pm 5.9\%$ of the scratch area after 48 h compared to $80.0 \pm 6.0\%$ for the sealant-protected group (Figure 3c; Figure S4a, Supporting Information). Fluorescence staining for live (calcein) or dead (propidium iodide) cells confirmed that the delay seen in growth in the unprotected group was attributed to delayed growth rather than cell death (Figure 3b).

To elucidate the mechanism driving the protection mediated by GastroShield, we evaluated the pH buffering capacity of the

biomaterial (Figure 3d). We added simulated stomach fluid (SSF, pH = 2) to the upper chamber of the transwell system daily and PBS to the bottom chamber covered with cells and monitored the pH in the model wound (bottom chamber) overtime (Figure 3e). When the simulated wound was protected with GastroShield, the pH of the bottom chamber (PBS) was not acidified, and its protective effect persisted for at least 1 week (Figure 3f). In the unprotected group, the pH steadily decreased as the SSF passed freely through the membrane over 24 h, reaching a minimum pH of 3.85 ± 0.05 (Figure 3f). Given the presence of PEI groups within GastroShield's network which are notoriously known to act as a proton sponge,^[57] we hypothesized that the protection from the low pH results from the sealant serving as a physical barrier, as well as exhibiting buffering capacity. To study this buffering capacity, we added incremental amounts of 0.5 M HCl to 200 μ L of GastroShield in 1 mL of PBS and compared it with 1 mL of PBS alone. After adding 20 μ L of 0.5 M HCl to PBS, its pH dropped to 3; while, GastroShield maintained a near physiological pH of 6.73. Overall, GastroShield was able to buffer up to 65 μ L to reach the same pH level of PBS following 20 μ L acid addition (Figure 3g; Figure S4b, Supporting Information).

We next investigated the ability of GastroShield to protect tissue from lytic enzymes, such as pepsin, that are found in the SSF at concentrations up to 1.8 mg mL⁻¹.^[55,58] We compared the "wound" side protection provided by a thin layer of freshly sprayed GastroShield or GastroShield exposed to SSF for 1 week and unprotected. Pepsin was labeled fluorescently (FITC) and added to the top of the transwells (Figure 3h). In the unprotected group, over 50% of the pepsin had crossed the membrane within 1 h. In the GastroShield-protected transwells (both fresh and aged), over 98% of the pepsin was blocked (Figure 3i). To mechanistically investigate how GastroShield shields from enzymes such as pepsin, we studied the penetration of pepsin into GastroShield gels overtime (Figure 3j). We observed that a thin layer of pepsin formed atop of the gel as early as 5 min post gel incubation that reached a penetration of ≈ 250 μ m in the following days (Figure 3k), suggesting minimal/no pepsin crossing, given the typical hydrogel thickness of ≈ 2 mm.

Taken together, these results indicate that GastroShield's sealing and proton-sponge capacity protect the wound from the acidic environment and from enzymes that delay wound healing processes.

2.3. GastroShield's Biocompatibility Meets the Highest Preclinical Standards

To investigate the level of cytotoxicity induced by the sealant, we treated cells with extracts obtained from GastroShield and other commercially available sealants following 24 h of incubation at 37 °C (Figure 4a). Formulations depicted varying toxicity levels for the different materials, with BioGlue exhibiting the most pronounced cytotoxicity ($19.6 \pm 1.2\%$ of cells remained viable 24 h after treatment) and GastroShield depicted the highest biocompatibility ($105.4 \pm 9.4\%$ cell viability). In addition, we performed biocompatibility assessment of several GastroShield formulations as well as the individual components (Figure S5a,b, Supporting Information). We found that reducing the solid content of oxidized dextran in the formulations further decreased the already

minimal cytotoxic effects of material extracts. We also confirmed minimal toxicity imparted by the precursor solutions (Figure S5c, Supporting Information), with polymers exhibiting a half maximal inhibitory concentration (IC₅₀) in the mg mL⁻¹ range (IC₅₀ = 20.67 mg mL⁻¹ for PluPEI and 2.53 mg mL⁻¹ for Oxidized Dextran).

We next assessed additional aspects of the biocompatibility of GastroShield in vivo, using a rabbit subcutaneous model. Rabbits were surgically implanted with precast hydrogels on day zero, and pathological responses, scored by a trained pathologist, were evaluated on days 14 and 28 (Figure 4b). Responses were evaluated in animals implanted with GastroShield versus sham controls (USP high density polyethylene [HDPE]) by assessing different degrees of inflammation, cell type infiltration, fibrosis, necrosis, and neovascularization. No significant differences in the biological response score were noted between GastroShield and control groups on days 14 and 28 post-implantation, with similar degrees of inflammation, lymphocyte, plasma cell, macrophage, and giant cell infiltration, necrosis, neovascularization levels, fibrosis, and fatty infiltrates (Figure 4c–e), validating GastroShield's subcutaneous compatibility.

We then sought to confirm the non-genotoxic potential of GastroShield. Genotoxicity was evaluated using the salmonella typhimurium reverse mutation assay (Ames), which assessed the number of mutations in genetically modified bacteria induced by the hydrogel extract, in comparison to positive and negative controls (Figure 4f), when incubated in polar (PBS) and non-polar solvents (DMSO) to extract water soluble and insoluble factors. Extraction was conducted for 72 h at 70 °C. Extract media were then applied to multiple bacteria strains that were genetically modified to portray histidine or tryptophan growth dependency. Hence, the number of colonies in groups treated with the extract (that also lacked tryptophan and histidine) would indicate bacterial mutagenesis. Bacterial cultures incubated with a pro-mutagen activator were used as positive controls. Each group was further tested in the presence or absence of rat liver S9 homogenate—a metabolic activator required based on the ISO 10993-3 guidelines. No evidence of mutagenicity/genotoxicity was noted in the polar and non-polar extracts of our sealant in the multiple bacterial strains tested (Figure 4g,h).

We studied the potential allergenic effect of our sealants using the Kligman sensitization study (Figure 4i). The test was used for assessing irritation and skin sensitization upon topical contact of animals previously injected with extracts obtained from preformed hydrogels (ISO 10993-10, Biological Evaluation of Medical Devices – Part 10). In brief, guinea pigs were injected on day 0 with extracts; and then, topically exposed to the same extracts on day 7 for 48 h, applied atop of the region in which the extract was injected on day zero; hence, favoring the induction of an allergic response. Animals were then re-challenged with secondary topical exposure of extracts, on days 23 and 24, and potential allergic reactions were recorded on days 25, 26, and 27. The animals were graded according to the reaction type (0 = no visible change, 1 = discrete or patch erythema, 2 = moderate and confluent erythema, and 3 = intense erythema and swelling) and according to the percentage of animals depicting an allergic reaction (0 = non-sensitization detected, 1 = weak sensitization [$<10\%$], 2 = mild

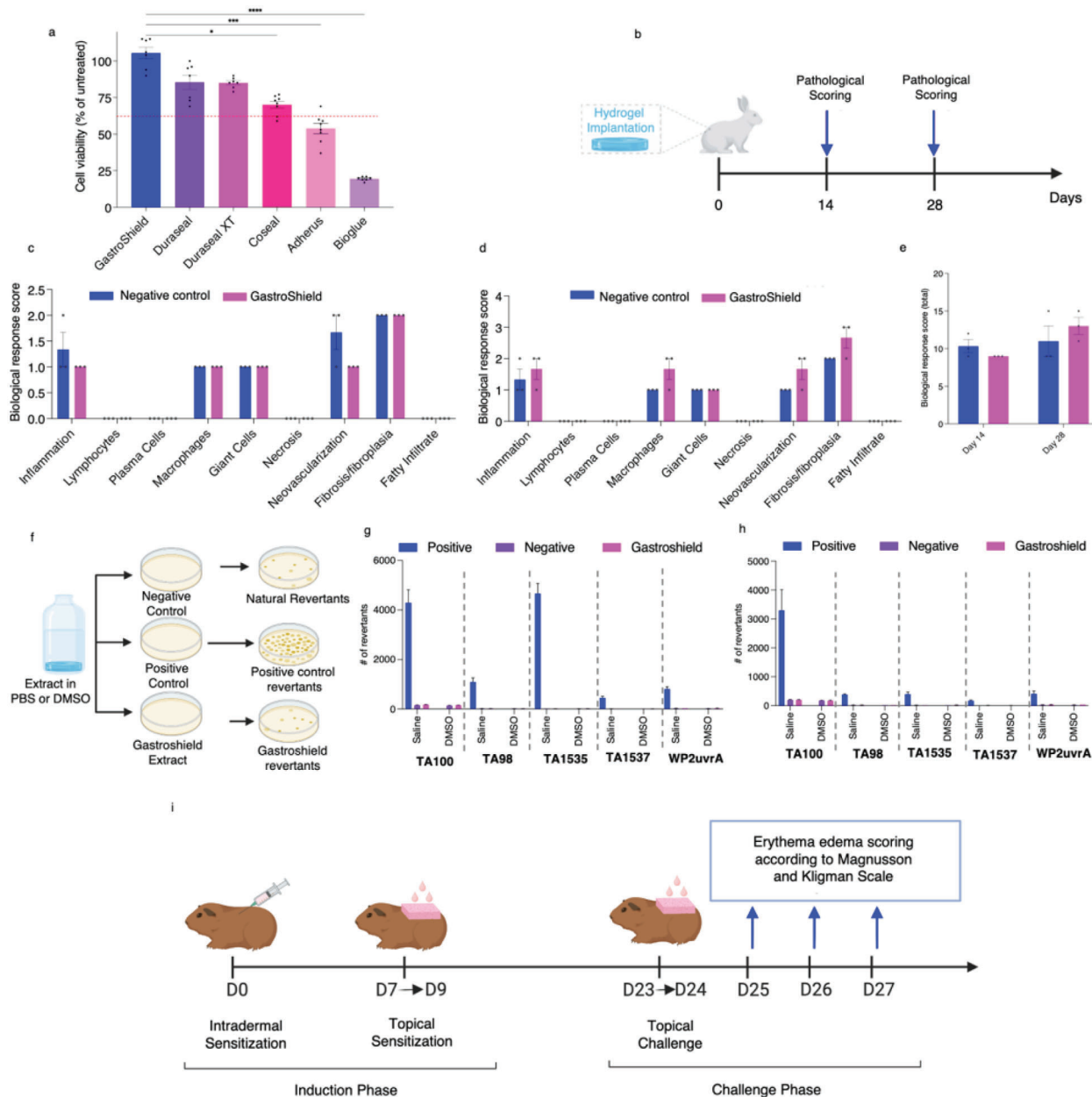


Figure 4. Biocompatibility studies in cell cultures and in large animals. a) Neutral red uptake assay for cell biocompatibility of GastroShield (10% Ox Dex:20% PluPEI) and a range of commercially-available materials. FDA establishes a threshold of 75% in cell viability for a material to be considered non cytotoxic, $n = 4, 7, 7, 8, 8,$ and 7 samples from left to right. b) Pathological scoring following subcutaneous biomaterial implantation in rabbits after 2 and 4 weeks. c) Individual scoring parameters of negative control ($n = 3$ samples) and GastroShield ($n = 3$ samples) at 2 weeks and d) 4 weeks. e) Overall biological responses to GastroShield after 2 and 4 week implantation period, $n = 3$ samples per group. f) Scheme of Ames genotoxicity test where the number of bacterial colonies for each strain (TA100, TA98, TA1535, TA1537, and WP2uvrA) is directly associated with the mutagenicity capacity of the material extract. g) Ames results display no difference between negative control and GastroShield in the non-metabolic activated test and $n = 3$ samples per group. h) Metabolic activated test, $n = 3$ samples per group. i) Guinea-pig sensitization assay following multiple applications of the material extract together with an adjuvant aiming to maximize any potential allergic reaction shows no sensitization effects for the GastroShield group. Data are expressed as mean \pm SEM; * $p < 0.05$, ** $p < 0.01$, *** $p < 0.001$, and **** $p < 0.0001$.

sensitization [10–30%], 3 = moderate sensitization [31–60%], 4 = strong sensitization [61–80%], and 5 = extreme sensitization [81–100%]). Using this setup and scoring system, the observed levels of sensitization for animals receiving the sealant extract were 0 for both reaction type and allergic reaction, thereby

suggesting the non-sensitization/irritation effect of the sealant in vivo.

Altogether, these results demonstrate the safety of the hydrogel and its byproducts, the non-inflammatory nature of the formulation, and safe profile in the context of genotoxicity.

2.4. GastroShield Achieves Sustained Protection Even in the Harsh Conditions of the Stomach

Achieving robust adhesion to the gastric lumen represents a remarkable challenge due to its mucus-rich surface, low pH environment, and catabolic agents. Hence, we studied the ability of GastroShield to be rapidly and effectively applied to a 2 cm laceration in an ex vivo stomach model, achieving instantaneous sealing and strong adhesion within 5 s (Figure 5a; Video S1, Supporting Information). To quantify the degree of adhesion, we employed a burst pressure (BP) test, which measured the maximum pressure required to rupture the perforated stomach when safeguarded by the sealant (Figure 5b).

The burst pressure test served two primary objectives—evaluating GastroShield's adhesion performance in comparison to various commercially available surgical adhesives (whose type and composition are depicted in Table S1, Supporting Information) and to assess the sealant's ability to maintain adhesion over time when exposed to physiologically relevant environments. Rapid loss of adhesion is in fact a major contributor to the failure of existing surgical sealants, resulting in delayed post-operative complications.^[17] We therefore compared burst pressure (BP) measurements obtained at t_{0h} and t_{24h} post-sealant application to the stomach ex vivo (Figure 5c).

GastroShield exhibited a burst pressure of 64.7 ± 11 mmHg at t_{0h} and 56.3 ± 12 mmHg at t_{24h} , demonstrating a minor decrease in the average BP, of $\approx 13\%$. In contrast, BioGlue, an FDA-approved material for vascular sealing, displayed 61% decrease in burst pressure (110.0 ± 50.1 mmHg at t_{0h} and 43.0 ± 37 mmHg at t_{24h}); Coseal, another FDA-approved vascular sealing agent exhibited 57% reduction in burst pressure (56.7 ± 45.5 mmHg at t_{0h} and 24.4 ± 29.9 mmHg at t_{24h}); Adherus, approved by the FDA for dura sealing, showed a drop of 40% (51.3 ± 26.7 mmHg at t_{0h} and 30.8 ± 21.3 mmHg at t_{24h}); and Duraseal Xact, also approved for dura sealing, resulted in a decrease of 43% in BP (55.0 ± 33.6 mmHg at t_{0h} and 31.3 ± 14.3 mmHg at t_{24h}). Duraseal and Tisseel were completely detached at t_{24h} (7.8 ± 3.3 mmHg at t_{0h} and 1.7 ± 0.5 mmHg at t_{24h} , respectively). To further evaluate the interfacial tissue–biomaterial interactions, fluorescence imaging was employed upon application and after 24 h to quantify the area of the tissue:material interface that was associated with changes in adhesion level.^[42] The interface between GastroShield (green) and stomach tissue (red) revealed minimal changes from t_{0h} to t_{24h} , suggesting that adhesion strength was maintained overtime (Figure 5d).

We next investigated the feasibility of endoscopically applying GastroShield (formulation 20%:20%) in a large preclinical animal model (pig), validating its instantaneous gelation and effective wound coverage in clinically-relevant conditions such as in the presence of a lesion (Figure 5e). The GastroShield spray was administered within 5 s (Figure 5f; Video S2, Supporting Information), resulting in adequate lesion coverage (lesions of 2 cm in diameter) (Figure 5g) and oozing control (Figure 5h) without off-target spraying or dripping. During necropsy examination, GastroShield effectively managed bleeding throughout the duration of the study, exhibiting strong adhesion. From the sample of nine lesions endoscopically sprayed with GastroShield, 100% of hydrogels was still adhered to stomach tissues at 6 h, 100% resisting finger rubbing, 56% resisting aberrant metal tool scrapping, and

44% resisting peeling, which was deemed adequate (Figure 5i; Figure S6, Supporting Information). Importantly, a common issue that may arise when applying two-part hydrogels is nozzle clogging after a short pause in the application.^[59,60] Our catheter was designed to avoid this issue as it didn't require a nozzle tip. The three circumscribed lumens allowed for a clogging-free spraying process.

2.5. GastroShield Ensures Protection in Colonic Lacerations Over Time

We next studied the ability of GastroShield to maintain colonic lesion protection over time, given the delayed bleeding seen following polypectomies.^[3,10] We investigated the BP achieved by GastroShield and other commercial materials immediately post application and after 24 h of incubation in physiological conditions (wet environment, 37 °C). The BP obtained could be directly correlated with the ability of the material to maintain tissue protection. The mean BP for GastroShield was 50 ± 18.8 mmHg at t_{0h} and 47.4 ± 16.8 mmHg at t_{24h} , representing 5% reduction within 24 h (Figure 6a). Besides the non-biocompatible BioGlue that depicted a 119.4% increase in adhesion at 24 h (15.5 ± 1.7 mmHg at t_{0h} and 34.0 ± 9.1 mmHg at t_{24h}), all other commercially available formulations portrayed significant reduction in BP over time: 14% reduction from 19.0 ± 9.3 mmHg at t_{0h} to 16.3 ± 6.2 mmHg at t_{24h} for Duraseal Xact; 50% reduction from 29.8 ± 13.0 mmHg at t_{0h} to 14.8 ± 1.6 mmHg at t_{24h} for Adherus; 75% reduction from 17.0 ± 8.4 mmHg at t_{0h} to 4.2 ± 4.1 mmHg at t_{24h} for Tisseel; 80% reduction from 25.0 ± 8.0 mmHg at t_{0h} to 5.0 ± 6.1 mmHg at t_{24h} for Duraseal; and 89% reduction from 57.8 ± 17.1 mmHg at t_{0h} to 6.5 ± 3.8 mmHg at t_{24h} for Coseal. We further measured the prolonged intestinal adhesion of GastroShield by fluorescence microscopy, by quantifying the hydrogel signal at the interface between the gel and tissue. Our analysis revealed a similar percentage of tissue surface covered with GastroShield at t_{0h} ($86.6 \pm 6.4\%$) and at t_{24h} ($81.0 \pm 5.0\%$) (Figure 6b; Figure S7, Supporting Information).

We next investigated GastroShield application in vivo when sprayed over colon lesions (2 lesions per animal) in pigs. The untreated control consisted of a spray with saline solution. At predetermined time points (days 1, 3, 7, and 14), two animals per group were sacrificed and the presence of GastroShield and the status of the lesion were examined (Figure 6c). The main goals were 1) to investigate whether the material remains adhered to lesions until they reach complete healing which significantly reduces the risk of post-operative complications such as delayed bleeding or perforation, and 2) to confirm that the adhesive material was not causing any unexpected adverse responses.

When examining adhesion at necropsy, 24 h post application, we found that 100% of the samples were still adhered to the colon mucosa, 100% resisted finger rubbing, 80% resisted metal scrapping, and 60% resisted metal peeling, pointing at a strong adhesion profile (Figure 6d). We further compared the GastroShield lesion coverage observed during endoscopic application to the coverage observed at necropsy and noted that 8/10 of samples depicted 100% coverage at endoscopic view which matched 100% coverage at necropsy. Surprisingly, we noted that two samples that exhibited minor degree of lesion coverage

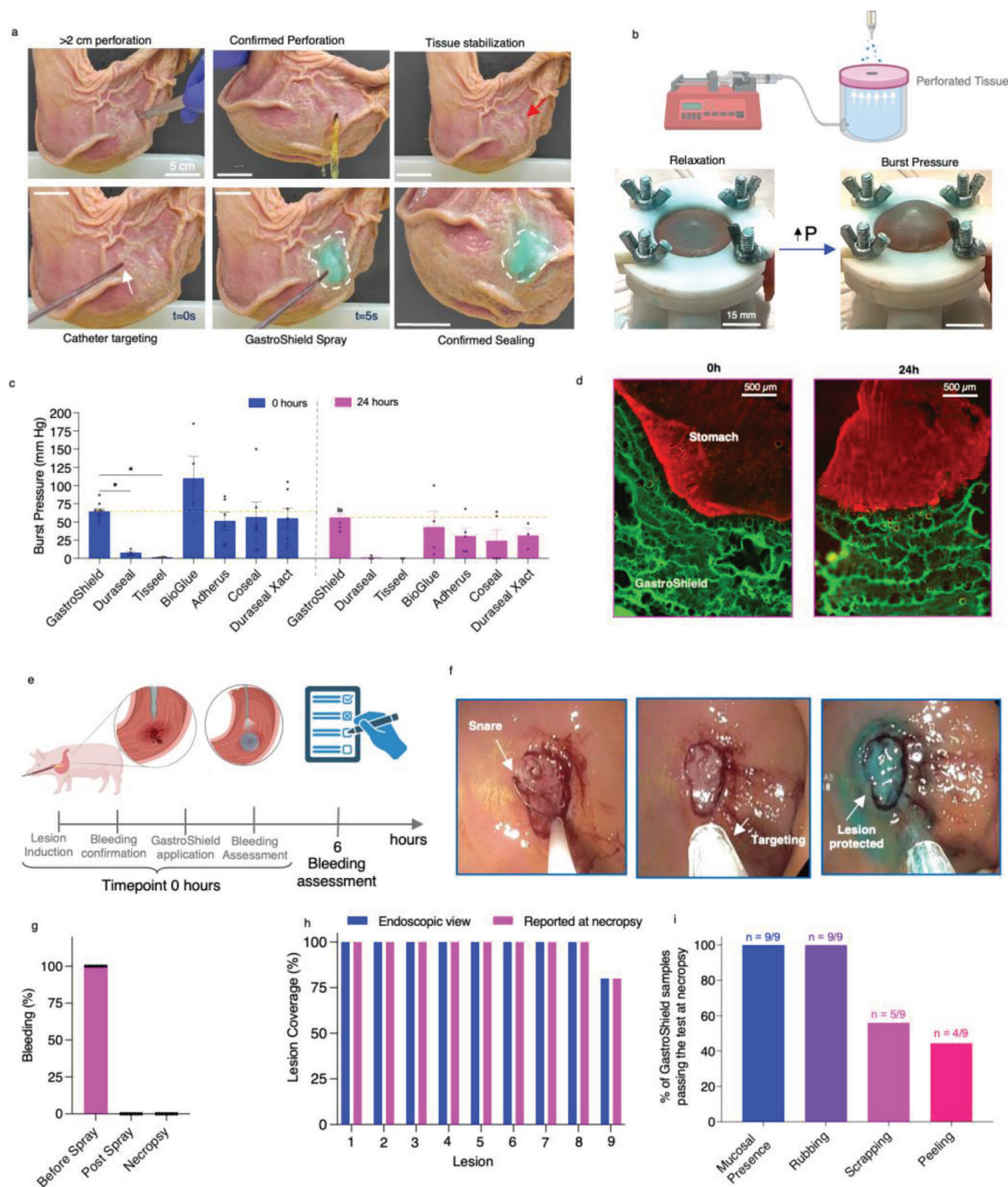


Figure 5. GastroShield exhibits a superior adhesion profile compared to commercial solutions and high levels of in vivo adhesion to stomach lesions. a) Ex vivo sealing capacity of GastroShield applied to porcine stomach mucosa with an ≈ 3 cm perforation. GastroShield was applied to the lesion and sealing was confirmed by measuring the liquid volume released when tilting the stomach that contained simulated stomach acid. b) Schematics of burst pressure of tissues perforated with a lesion of 3 mm in diameter. Pressure was measured with a pressure sensor until burst. c) Burst pressure obtained for GastroShield and competitor materials at t_0 and t_{24} h post application to stomach lesions (From left to right, $n = 9, 7, 4, 6,$ and 6 at 0 h and $7, 3, 4, 5,$ and 5 at 24 h). d) Fluorescence imaging (FITC = hydrogel; Texas Red = tissue) revealed similar tissue–biomaterial interaction adhesion profiles at 0 and 24 h post incubation in acidic conditions (pH = 2, 37 °C). Scale bar = 500 μm . e) In vivo study timeline comprising of an induced stomach bleeding followed by endoscopic spraying of GastroShield or Saline. Immediately after application and 6 h post-intervention, necropsy was performed. f) Images of in vivo endoscopic intervention (left), catheter placement and focusing (middle), and GastroShield application (right). g) Bleeding was effectively controlled following GastroShield application, as confirmed at necropsy. $n = 8$ lesions per group. h) Lesion coverage comparison between the endoscopic view and “real” view following necropsy. i) Percentage of GastroShield–tissue samples passing the following tests at necropsy (at 24 h): Mucosal presence of GastroShield; material is adhered but it can be detached with strong finger rubbing; material detaches under metal tool scraping or can only be removed with peeling it from underneath with metal tools, $n = 9$ lesions in total. Data are expressed as mean \pm SEM; * $p < 0.05$, ** $p < 0.01$, *** $p < 0.001$, and **** $p < 0.0001$.

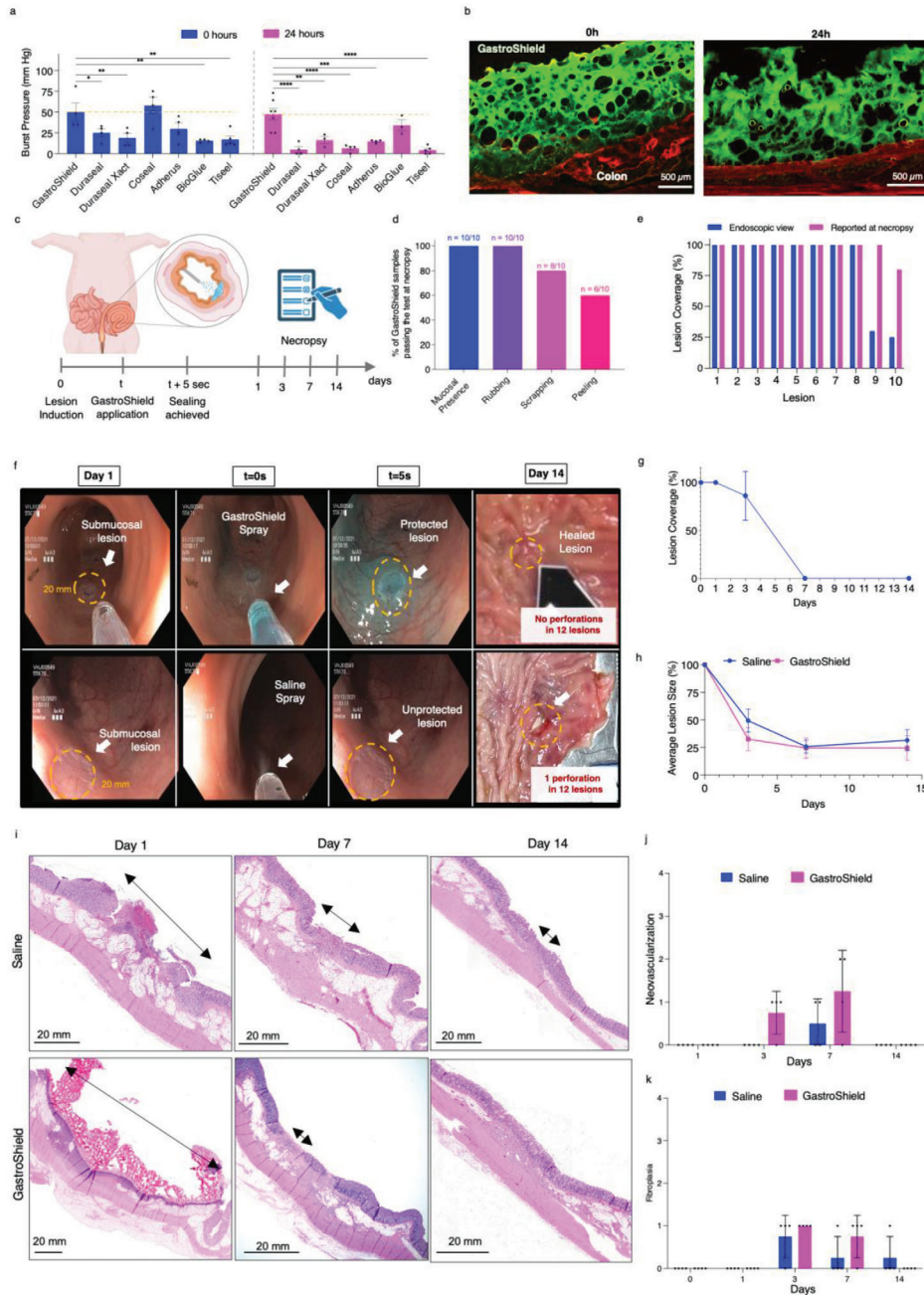


Figure 6. GastroShield exhibits high level of adhesion to colonic tissues in vitro and in vivo, without interfering with the natural wound healing profile. a) Burst pressure obtained for GastroShield and commercially available materials at t_0 and t_{24} h post application to colonic lesions. From left to right, $n = 4, 4, 5, 4, 4, 4, 4, 4$ at 0 h and 7, 4, 5, 3, 4, 4, and 3 at 24 h. b) Fluorescence imaging (FITC = hydrogel; Texas Red = tissue) revealed similar tissue:biomaterial interfaces at t_{0h} and t_{24h} . Scale bar equals 500 μm. c) In vivo timeline initiated by lesion induction followed by GastroShield or Saline endoscopic spraying on day 0, and necropsy on days 1, 3, 7, and 14. d) Percentage of GastroShield-tissue samples passing the following tests at necropsy (at 24 h): mucosal presence of GastroShield; material is adhered but it can be detached with strong finger rubbing, material detaches under metal tool scraping and if material can only be removed by peeling it from underneath with metal tools, $n = 10$ lesions analyzed. e) Comparison of lesion coverage by endoscopic view and during necropsy—24 h post GastroShield application. f) Images of in vivo endoscopic application of GastroShield (top) or saline (bottom). g) Lesion coverage (% of lesion area) assessed at necropsy at different timepoints, $n = 3, 4, 4, 4$ lesions analyzed for timepoints 1, 3, 7, and 14 days, respectively. On day 3, 100% of lesions had GastroShield presence. GastroShield presence was not found on Days 7 and 14. h) Average lesion size measured at necropsy, $n = 12, 4, 4, 4$ lesions for timepoints 0, 3, 7, and 14 days, respectively for Saline group and $n = 13, 2, 4, 4$ for timepoints 0, 3, 7, and 14 days, respectively for GastroShield group. i) Histological images of lesions at different timepoints: day 1 (left), day 7 (middle), and day 14 (right). Scale bar equals 20 mm. Arrows depict the lesion size. j) Neovascularization scoring provided by a trained pathologist during necropsy, $n = 4$ lesions/group/timepoint. k) Fibroplasia scoring (which refers to growth or proliferation of fibrous tissue as a marker of lesion healing) provided by a trained pathologist, $n = 4$ lesions/group/timepoint. Data are expressed as mean \pm SEM; * $p < 0.05$, ** $p < 0.01$, *** $p < 0.001$, and **** $p < 0.0001$.

during endoscopy were found in fact to portray higher coverage at necropsy—100% (necropsy) instead of 25% (endoscopy) and 75% (necropsy) instead of 20% (endoscopy) for lesions 9 and 10, respectively (Figure 6e), suggesting that even a thin layer of GastroShield can adhere to and protect the mucosal tissue.

We next studied the *in vivo* prolonged adhesion of GastroShield in colon lesions up to 14 days post application (Figure 6f). We found that GastroShield was found in 100% of sprayed lesions at day 3 post-hydrogel application, with average lesion coverage of more than 80% of the lesion area in the same timepoint, followed by decreased persistence by day 7 (Figure 6g; Video S3, Supporting Information). Importantly, we confirmed that GastroShield application does not interfere with the natural wound healing process as observed by a comparable reduction in lesion size in wounds applied with GastroShield or with Saline (Figure 6h).

We also confirmed that the fast gelation of the material prevents undesired luminal adhesion to the opposite wall, even when peristaltic movements are present (Video S4, Supporting Information). We hypothesize that the new tissue (mucosal layer) formed beneath the hydrogel layer caused material detachment (Figure 6i). Yet, this is an interesting feature that deserves further investigation. It seems that as the tissue was protected for a few days and allowed to heal (hence, the risk of bleeding becomes minimal), the material was delaminated as a new mucosal layer was formed. During necropsy, at day 7, we found the entire hydrogel among the feces on multiple occasions, indicating that it was detached from the tissue. No remains of hydrogel were found on day 14, indicating facile elimination of the bulk hydrogel via feces. Inflammatory analysis performed by a certified pathologist revealed that the levels of neovascularization in the group treated with the sealant started to manifest at day 3 post-treatment, whereas signs were noted only on day 7 in the group treated with saline (Figure 6j). We also observed that GastroShield-treated tissues depicted similar levels of fibroplasia (Figure 6k), necrosis (Figure S8a, Supporting Information), and inflammation (Figure S8b, Supporting Information), suggesting the ability of GastroShield to allow the natural body healing mechanism to occur via the wound shielding.

No perforations were noted in the early timepoints of the study (Figure 6f), though one instance of perforation on day 14 was found in the control group; while, none were found in the GastroShield-protected group. Due to the low incidence, there was no statistically significant difference between the groups. Interestingly, this level of incidence was in agreement with reported clinical level of complications that result with severe patient outcomes.^[16] Additional studies are required to increase the statistical power of this observations, but this event supports the use of the swine model for validating material performance in clinically relevant scenarios.

To further elucidate how GastroShield application can be advantageous in the context of hard-to-treat perforated lesions, we conducted a separate study in which we applied GastroShield onto colonic perforations undergoing standard metallic clipping (Figure S9, Supporting Information). In this challenging model, we observed that GastroShield application effectively sealed clipped perforations, with hydrogel presence detected in 33% lesions 7 days post GastroShield application.

3. Outlook

Gastrointestinal complications such as bleeding and perforations can arise naturally as in the case of advanced ulcers or from lesions created by interventional procedures such as polyp or tumor removal. The current solution for controlling these post-procedural complications is closure via metallic clips,^[23] which were developed in 1975^[61] and are challenging to apply, expensive, time consuming, and rarely prevent post-operative bleeding.^[24–26] Currently, there is no material-based solution that is able to prevent post-operative complications as best alternative options work only in active bleeding or only achieve mucosal adhesion for less than 1–2 days.^[17]

To address this unmet challenge, we investigated the ability of GastroShield to achieve high mucosal adhesion, high biocompatibility, and prolonged sealing capacity that would last a few days post application onto GI wounds. This would protect the tissue during the critical time when complications occur and allow the natural wound healing mechanism to take place. GastroShield is formed by the reaction between self-assembled Pluronic micelles made of amine-modified block-copolymer (PluPEI) with oxidized dextran, which enable immediate covalent cross-linking augmented by ionic interactions. In preclinical EMR/ESD animal models that replicate clinical conditions, GastroShield demonstrated remarkable retention rate of 100% in colonic tissues for at least 72 h and up to 7 days in 33% of hard-to-treat perforated lesions, without affecting the natural wound healing process—a milestone that to the best of our knowledge has not been previously described in the literature for these types of technologies.

Hydrogel mucosal adhesion and persistence following application are influenced by numerous interactions within the polymeric network itself and between the hydrogel and the tissue. The choice of amine modified-Pluronic as cross-linkers is found to be highly advantageous as they expose multiple amine-groups in its micellar conformation, which enables for fast reaction with dextran aldehyde and network formation. In addition, it confers mechanical strength to the hydrogel by dissipating energy upon peristaltic stresses via disruption and reassembly of the micelle structure; while, keeping the network's imine groups and hydrogel mechanical properties intact.^[62,63]

To achieve prolonged tissue adhesion, GastroShield capitalizes on complementary tissue:biomaterial interaction mechanisms. These include covalent imine bond formation between material aldehyde groups and tissue amines, hydrogen bonds, and ionic interactions between the amine-rich polymer matrix and tissue amine and carboxylic acid groups, as well as interdigitation of polymeric chains into the tissue. These complimentary interactions enable GastroShield to achieve exceptional and prolonged adhesion, even under the harsh conditions in the GI tract. In the studies presented here, GastroShield outperformed six commercially available materials and matched the adhesive strength of BioGlue, the market's strongest material, without exhibiting its associated high toxicity. Importantly, GastroShield presented excellent biocompatibility, meeting ISO 10993 FDA guidelines for cytotoxicity, guinea pig sensitization, genotoxicity, and rabbit 30-day subcutaneous implantation, thereby enhancing its clinical translation potential.

Hydrogel formulations designed for GI applications have been reported in the past.^[17,33–37] However, they broadly fall short

of maintaining adequate performance over time (from a few hours to 48 h) and some require multiple steps that involve toxic reagents (i.e. sodium periodate),^[37,38] precluding them from clinical adoption. Imine-bond forming hydrogels have been reported for other applications (e.g., antibacterial, vascular). These include an amine-modified PEG-Oxidized dextran hydrogel,^[42] as well as polyamidoamine dendrimer-based oxidized dextran hydrogel sealant.^[27] Another example is a fast-gelling two-part injectable adhesive hydrogel based on oxidized dextran solution and PEI solution.^[64] While these studies offer advantages in the context of achieving high adhesion, they suffer from critical drawbacks that limit their adoption in gastrointestinal applications because these materials are created via the conjugation of a polysaccharide (i.e., dextran) with a rigid macro-crosslinker (i.e., dendrimer or PEI) that cannot dissipate energy, unlike the PluPEI micelles. Further, some of these formulations exhibit cytotoxic properties such as free, high molecular weight PEI that is highly cytotoxic and limits their wide adoption. Perhaps most importantly, these formulations exhibit viscosities that are incompatible with long-catheter mediated delivery during an endoscopic application.

Novel technologies based on hemostatic powders have been commercialized as well.^[39,65] These powders can be readily sprayed via a catheter but they don't achieve satisfactory tissue adhesion and rely on hydration to form a coating layer which can induce heterogeneous coating. This may be the cause of early material detachment and bleeding, as early as 6 h post application, with more than 50% of the tissues not exhibiting the sprayed powders 42 h following application.

Overall, GastroShield provides a robust, thin coating of GI lesions of varying sizes and shapes within seconds. We have demonstrated this in vitro and in challenging in vivo large animal preclinical models, where GastroShield effectively protected the underlying tissues against harsh environment; while, maintaining high and prolonged adhesion. It adhered strongly to mucosal and submucosal tissues, even in the presence of blood, mucus, and moisture for up to 7 days, with the ability to be used also in conjunction with standard of care methods such as metallic clips, if needed. This underscores its potential to transform the toolkit available for clinicians to manage internal surgical procedures. By identifying the considerations and key design parameters, our approach can set the stage for future development of biomaterials for minimally invasive surgical procedures, especially for managing wounds in traditionally challenging-to-seal tissues.

Next, we will further investigate the ability of GastroShield to protect gastric wounds in a chronic setting. We anticipate that by creating a hydrogel coating that shields the lesion from the acid and gastric enzymes, wound healing will be significantly improved. Additional studies required for translation to clinical practice^[67] will focus on conducting usability studies, which become critical to assure broad adoption of the technology by endoscopists.

4. Experimental Section

Synthesis of Oxidized Dextran: Aldehyde groups were introduced into dextran polymers via sodium periodate oxidation. 160 mL of deionized water containing 19.6 g of dextran was activated via dropwise addition of a solution containing 17.8 g of sodium periodate dissolved in 170 mL of deionized water under continuous stirring. The solution was left at room

temperature for 5 h. Then, the oxidized polymer was transferred to dialysis membranes (3.5 kDa molecular weight cutoff [MWCO], Repligen) and left for 4 days with daily changes of water. Next, the purified oxidized dextran was frozen to $-80\text{ }^{\circ}\text{C}$ and lyophilized until completely dry. The successful chemical modification of oxidized dextran was confirmed by NMR-H and FTIR spectroscopy.

Synthesis of PEI-Modified Pluronic f68: Pluronic-f68 was modified via the addition of amine groups using 1,1'-Carbonyldiimidazole (CDI) activation of alcohol groups on the polymer terminals and reaction with polyethylene imines (PEI, 600 MW, Sigma-Aldrich), as previously described.^[68] In brief, 50 mL of acetonitrile (ACN) containing 16.8 g of Pluronic-f68 was activated overnight via dropwise addition of an ACN solution (40 mL) containing 3.25 g of CDI. On the next day, 32.0 g of PEI was dissolved in 40 mL ACN and dropwise added to the activated solution of Pluronic-f68. The solution was left at room temperature under vigorous stirring overnight. In the following day, ACN was evaporated from the polymer solution ($40\text{ }^{\circ}\text{C}$ and pressure = 90 mBar) and solubilized in 100 mL of deionized water. The solution was then transferred to dialysis membranes (3.5 kDa molecular weight cutoff [MWCO], Repligen) and left for 12 days with changes of water every 3 days. Next, the purified modified polymer solution was frozen to $-80\text{ }^{\circ}\text{C}$ and lyophilized until completely dry. The successful chemical modification of oxidized dextran was confirmed by FTIR spectroscopy and NMR-H.

Gelation Time: Gelation time was measured by combining 100 μL of each component in an inverted cap of a 1.5 mL Eppendorf tube. In experiments investigating the effect of temperature in the gelation time, each precursor solution was kept at $37\text{ }^{\circ}\text{C}$ or room temperature until gelation.

Swelling, Water Content, and Stability Studies: Gel fraction and swelling were studied following 24 h of hydrogel fabrication (dimensions $10\text{ mm} \times 10\text{ mm} \times 2\text{ mm}$). To calculate the swelling, hydrogels were created by mixing 100 μL 50% oxidized dextran with 100 μL of PEI-modified Pluronic-F68. Then hydrogels were moved into a 24-well plate containing 1000 μL of $1 \times \text{PBS}$ per well. The plate was then placed in a $37\text{ }^{\circ}\text{C}$ incubator at 200 rpm. Following 24 h, swelling was calculated using the following formula:

$$\text{Swelling (\%)} = (W_{t_1} - W_{t_0}) / W_{t_1} \quad (1)$$

where W_{t_1} is the wet mass of the hydrogel at time t_1 and W_{t_0} is the initial wet mass of the hydrogel following fabrication. To calculate the total content of water in the gels, the following formula was used:

$$\text{Water Content (\%)} = (W_{t_1} - W_{d_{t_1}}) / W_{t_1} \quad (2)$$

where $W_{d_{t_1}}$ is the mass of the dry polymer after lyophilization. To calculate the stability of the gels following incubation at $\text{pH} = 7$ (PBS) and $\text{pH} = 2$ (pH adjusted PBS), multiple identical hydrogels (dimensions $10\text{ mm} \times 10\text{ mm} \times 2\text{ mm}$) were synthesized and incubated in the relevant buffers. At each timepoint, hydrogels were collected and lyophilized and weighed. Then, stability (%) was calculated as a fraction of dry weight at timepoint t_1 divided by the dry weight of gels immediately after fabrication (t_0).

Compressive Strength and Tensile Adhesion Strength Testing: Pre-casted GastroShield gels (100 μL of oxidized dextran with 100 μL of PEI-modified Pluronic-F68) were first synthesized and allowed to react for 5 min. Then, gels were either used for measurement of compressive strength or incubated for 24 h at $37\text{ }^{\circ}\text{C}$ for the same measurement. Measurement of the compressive strength (Instron Tensile Tester 5942) was performed at a rate of 0.05 mm s^{-1} and the stress and strain at break were measured. GastroShield toughness was calculated by computing the area under the curve of the stress-strain curves. Young's modulus was computed by measuring the tangent of the stress curve from 0% to 5% strain. To measure the adhesion strength of the material, the 10% or 20% Oxidized Dextran: 20% PluPEI formulations were mechanically tested with gelation time tuned to $\approx 20\text{ s}$ (pH adjusted to 7.6) using a mechanical tester (TA.XTPlus 100, Texture technologies). The utilized method was an adaptation of the ASTM F2258 "Standard Test Method for Strength Properties of Tissue Adhesives in Tension,"^[69] based on the analysis of a flat contact cylinder (0.5 cm^2) to the hydrogel followed by its adhesive measurement via probe pulling. A rectangular flat colon tissue was fixed on the mechanical tester plat-

form while another tissue was fixed and fully covered the flat surface of the probe. Then, ≈ 0.8 mL of hydrogel was applied on top of the tissue positioned at the base of the machine. The tissue-containing probe was then lowered until contact with the hydrogel. The probe was kept still for 600 s, allowing for gel curation. Then, the probe was raised at 5 mm s^{-1} . The adhesion strength was then measured following probe pull up.

Rheological Characterization: Rheological measurements using a Rheometer (TA Instruments, HR 20) were acquired to characterize the viscosity, storage modulus (G'), and loss modulus (G'') of the sealant precursor solutions as well as the lubrication effect promoted by the gel. To measure viscosity, G' and G'' , 500 μL of polymer solution was first loaded onto a dedicated plate (TA Instruments HR 20 Discovery Hybrid Rheometer). Then, the shear rate ($1/s$) was changed from 1 to 1000; while, the temperature was controlled at either 25°C or 37°C . Acquisition was performed via collection of five points per decade. To measure the lubrication of the gel in comparison to ex vivo tissue, a 20 mm diameter plate was sprayed with 1 mL of sealant, and then, incubated in PBS for 10 min prior to use. The sprayed plate was mounted atop of the rheometer and lowered until achieving 2 N of force against the sealant. The gel was pressed against a wet glass slide. Then, the torque was measured as a function of shear rate. The obtained results were converted to friction coefficient using the following formula:

$$\mu = \frac{1.5 \times \tau}{R \times F} \quad (3)$$

where μ is the coefficient of friction, τ is the measured torque, F is the loaded force, and R is the radius of the used plate. The same experiment was conducted for an ex vivo colon tissue completely covering the 20 mm plate.

Burst Pressure: To measure the pressures required to burst a sealant applied atop of a tissue perforation, fresh porcine colon and stomach tissues were cut into pieces of $\approx 50 \text{ mm} \times 50 \text{ mm}$. Then, a circular perforation was performed in the center of the tissue using a 3 mm biopsy punch. The prepared tissue was then placed in a tissue holder and fixed using a custom design cover. About 1 mL of sealant was sprayed atop of the tissue and left to react for ≈ 5 min. Then, the pressure was increased in the circuit by a syringe pump at 10 mL min^{-1} . The pressure was real-time measured by a PendoTECH pressure sensor, and the maximum pressure at burst was registered. This test was implemented 15 min following GastroShield application to fresh tissues or to tissues that were kept at 37°C for 24 h in a moisturized bag.

Fluorescent Labeling of Pepsin and GastroShield Shielding: Pepsin was fluorescently labeled with a fluorescein isocyanate (FITC)–fluorophore (ThermoFisher) following the manufacturers protocol. Labeling was performed by the dropwise addition of 2 mL of a FITC 2 mg mL^{-1} solution in DMSO to a 10 mg mL^{-1} pepsin solution in water. The solution was left overnight reacting at dark, 4°C . Then, the solution was dialyzed for five consecutive days in water. Lastly, FITC-pepsin was lyophilized and stored at -80°C until use.

GastroShield Shielding Transwell Experiments: FITC-labelled pepsin was used for the assessment of the sealing effect promoted by GastroShield applied atop of transwell inserts (six wells per plate). To that, pepsin solution (1.8 mg mL^{-1}) was added atop of inserts sprayed with 2 mL GastroShield. The lower chamber was filled with PBS and its fluorescence was measured over time. The plate was incubated at 37°C and in the dark. Pepsin depth penetration inside the hydrogel surface was also assessed overtime at different timepoints (5 min, 24, 96, and 168 h). Fluorescence penetration was assessed using a fluorescence microscope (Leica Microsystems) and processed using ImageJ. Depth of pepsin penetration was obtained via calculation of the full width at half-maximum (FWHM) of FITC signal at the interface between the hydrogel and the pepsin solution.

Wound Healing Assay: To mimic the recovery of cells in acidic environment (i.e., stomach) following the induction of a lesion with and without a sealant, six-well transwell plates were first seeded with 100×10^3 cells per well and allowed to grow for 48 h. A subset of inserts was sprayed with 1.2 mL of hydrogel, completely sealing the membrane that served as an interface between the cells (L929 murine fibroblasts; Sigma–Aldrich) and

the upper chamber of the insert. The gels were first allowed to fully cure in 10% FBS DMEM for 24 h at 37°C before the assay day. On the assay day, each well of the plate was first scratched using a 1 mL pipette tip horizontally. Next, the media of each well were exchanged to 1.45 mL of fresh media. Then, relevant wells were added with either hydrogel-sprayed inserts or no inserts. Next, 1 mL of “SSF-media” (10% FBS DMEM media pH-adjusted to 1.8) was added to either each insert or well. Phase-inverted microscopy was used as a mean to register the thickness of the scratch on multiple timepoints until recovery (0, 24, and 48 h). On the timepoint 48 h, cells were stained using Calcein AM (for live cells; Corning) and propidium iodide (for dead cells, MP Bio), using the manufacturer’s standard protocol for staining.

Fluorescent Imaging and Adhesion of GastroShield Applied to Tissues: Fluorescent imaging was conducted for the confirmation of GastroShield adhesion to colonic and stomach tissues. Tissues were sprayed with ≈ 2 mL of GastroShield and paraffin-mounted immediately or 24 h post incubation at 37°C in the dark. In the case of stomach tissues, sprayed tissues were kept in acidic environment ($\text{pH} = 2$) for the 24 h timepoint. In the case of colons, tissues were kept in PBS for the 24-h timepoint. Tissues were cryo-sectioned into $60 \mu\text{m}$ sections and immediately mounted onto glass slides. Staining was performed following manufacturer’s guidelines (Invitrogen) via embedding the sectioned tissue-loaded glass slide into a rhodamine phalloidin staining for 5 min before imaging. To calculate the percentage of tissue coverage with GastroShield at different timepoints, lines were traced using ImageJ software immediately above the interface between the tissue and the hydrogel, and the percentage of the line that exhibited values of at least 50% higher than baseline (likely indicating the presence of the sealant) was calculated.

Swine Stomach In Vivo Model: Four Yorkshire swine underwent lesion creation in two locations in the stomach per animal. Cold snare was used in conjunction with grasping forceps to create a stomach ulcer of $\approx 20 \text{ mm}$ with an active bleeding. GastroShield was sprayed after bleeding confirmation and the wounded area was observed for a few minutes to confirm proper wound protection and bleeding control. About 6 h after material application, the necropsy was performed and the presence and adhesion score of GastroShield evaluated over the wounded tissue.

In Vivo Adhesion Score: As conventional adhesion evaluation techniques are not compatible with the heterogeneous samples obtained from in vivo studies, a scoring system that enabled the adhesion quantification of GastroShield samples adhered to mucosal tissues was developed, as described in Figure S6, Supporting Information. The scoring method was to assign 0 score if there was no adhering material to the lesion, Score 1 if the material adhered but could be detached with strong finger rubbing, Score 2 if the material detached under metal tool scraping, and Score 3 if the material could only be removed peeling it from underneath with metal tools.

Swine Colon In Vivo Model: Sixteen male Yorkshire swine underwent lesion creation in up to three locations in the colon per animal by injecting saline lift solution into the submucosal space and using an electro-surgical generator to perform en bloc mucosal resection. Piecemeal resections were performed as needed at the same site to attain sufficient lesion size. GastroShield or control was administered over the lesion sites. In control animals, saline was sprayed over the lesion sites. Animals were survived following procedures. Animal health was monitored, including clinical observations, body weights/condition, and clinical pathology, at pre-determined, regular intervals. Animals were euthanized on Days 1, 3, 7, and 14 as applicable to the group. A necropsy was performed to grossly evaluate test material presence and adherence; size and location measurements relative to lesion site, mesenteric lymph nodes (MLNs), and spleen, were obtained. Treatment sites and two representative MLNs were harvested and divided for histopathology processing. The same procedure described above was adopted for studies involving perforated lesions, which were created using snare resections crossing the outer colonic serosa layer. Then, lesions were applied with one or two metallic clips to simulate the clinical perforation-closing scenario. Clip sealing was not water tight, which served for the authors’ assessment of GastroShield sealing and persistence onto lesions. Necropsy was performed 3 and 7 days post hydrogel application of colonic lesions.

The swine studies were performed at CBSET (Lexington, MA), accredited by AAALAC International, and committed to complying with all applicable regulations governing the care and use of laboratory animals. The studies were performed under the approved IACUC protocol Number I00322.

Statistical Analysis: Data in this manuscript are described as mean values \pm SEM. Graph Prism software was used to plot the data. Pairwise comparisons were computed using non-parametric unpaired Student *t*-test (Mann–Whitney test). Multiple comparisons between groups were determined using one-way ANOVA (Kruskal–Wallis test). In experiments reporting several groups per timepoint, the two-way ANOVA test was used and Dunnett's multiple comparisons test, with a single pooled variance. No specific pre-processing of data was performed prior to statistical analyses. Statistical differences among groups were considered significant if *p*-values were below 0.05 (**p* < 0.05, ***p* < 0.01, ****p* < 0.001, and *****p* < 0.0001). Some Illustrations displayed in this manuscript were prepared using the BioRender software.

Viability Studies: The cell viability studies performed in this manuscript were performed following the FDA recommendations for evaluation of safety of medical devices (ISO 10993–5). Specifically, the neutral red uptake (NRU) test, a test that is based in the lysosomal accumulation of neutral red (NR) dye, was used for viability quantification. The experiments were performed using L929 mouse fibroblasts. To study the effect of the extracted media of hydrogels, all precursor materials were sterilized via filtration 0.2 μ m filter (ePTFE, 0.2 μ m, 13 mm Cytiva Whatman Uniflo Syringe Filters). Then, 1 mL (\approx 1 g) of sealant was casted onto a sterile cylindrical mold and placed in a 15 mL sterile tube containing 5 mL of 10% FBS DMEM media. The sealant was incubated at 37 °C for 24 h, and then, used as a treatment to cells plated in 96-well plates (10×10^3 cells per plate). Following 24 h of incubation, the polymer-containing media was substituted by 100 μ L of NR-containing media (40 μ g mL⁻¹). Cells were then kept for 2 h at 37 °C, period in which viable cells incorporate the neutral red dye into their lysosomes. After that, the wells were washed three times with PBS to completely remove NR from the media. Lastly, 150 μ L of distain solution composed by 50% ethanol, 49% deionized water, and 1% glacial acetic acid was used to extract the dye incorporated by live cells. The OD of the neutral red extract was then measured at 540 nm using the SpectraMax i3x plate reader from Molecular Devices. To study the viability of the precursor reagents of the sealant, polymers were dissolved in DMEM containing 10% FBS and applied onto wells as treatment (200 μ L per well). To quantify the viability, the same procedure as the one described above was adopted.

Kligman Sensitization Study: To investigate the potential allergenic reaction induced by the authors' hydrogel application, Hartley guinea pigs were used (20 experimental, 10 negative control, and 5 positive controls). Hydrogel extract was obtained by extracting 200 mg of hydrogel mL⁻¹ of polar (USPO, 9% Sodium Chloride for injection) or non-polar (cottonseed Oil "CSO") eluents, for 24 h at 70 °C. Polar extraction mimicked the body conditions to extract leachable that would be released from the sealant in polar environment, as most tissues are in the body. The non-polar extraction, using CSO, mimicked the leachable that would be released from the sealant in non-polar body tissues such as fat. The study began with an induction phase (Day 0) where the sealant extract and controls were injected intradermally. The topical application phase (Day 7) was conducted by applying the sealant extract or control for 48 h at the site of the intradermal injections. On day 23, the challenge phase was performed by topically applying the extract and grading the erythema and edema at 24, 48, and 71 h post-challenge application.

Reverse Mutation Ames Genotoxicity: To detect reverse mutations within the histidine or tryptophan operon, the reverse mutation Ames genotoxicity assay was used. This assay analyses the induction of mutations in the histidine independent growth (*S. typhimurium*) or tryptophan independent growth (*Escherichia coli*). Sealant extraction was performed in polar (NaCl) and nonpolar (DMSO) solvents that were kept at 50 °C for 72 h. Multiple bacteria strains were exposed to the extracts via plate incorporation, in the presence or absence of metabolic activation. The number of colonies formed following 48 h of incubation at 37 °C was quantified for the assessment of the mutagenic potential of the material extract. For

each strain and condition, the numbers of colonies after exposure to the test article were compared to those of a negative control. The test article was considered not mutagenic if the difference was found not statistically significant (*p* > 0.05) to the negative control.

Ethics Statement: L-929 cells were purchased from ATCC. All in vivo (Yorkshire Pigs, Male Age 4 months, 45.2–62.6 Kg) experiments were conducted at CBSET. CBSET, Inc. is accredited by AAALAC International and is committed to complying with all applicable regulations governing the care and use of laboratory animals. All procedures and conditions of testing were in compliance with the USDA and AWA1/AWR2.

Supporting Information

Supporting Information is available from the Wiley Online Library or from the author.

Acknowledgements

G.M.T. and D.D. contributed equally to this work. The authors appreciate Dr. Nick Collela's help with the mechanical characterization of the developed sealant. The authors would like to thank the National Science Foundation (NSF) for the funding provided (2335845). The authors thank the CBSET staff and study director Jay Budrewicz for their support with pre-clinical studies.

Conflict of Interest

G.M.T., N.A. and E.E. are inventors on the patent describing the bioadhesive. G.M.T., D.D., N.A. and E.E. are employees or advisors of BioDevek Inc, a medical device company focused on the development of surgical biomaterials.

Data Availability Statement

The data that support the findings of this study are available in the Supporting Information of this article.

Keywords

gastrointestinal, hydrogel, polyp, protection, sealant, wound protection

Received: November 7, 2023

Revised: February 13, 2024

Published online: April 1, 2024

- [1] M. Arnold, C. C. Abnet, R. E. Neale, J. Vignat, E. L. Giovannucci, K. A. McGlynn, F. Bray, *Gastroenterology* **2020**, *159*, 335.
- [2] National Cancer Institute Staff, Why Is Colorectal Cancer Rising Rapidly Among Young Adults?, <https://www.cancer.gov/news-events/cancer-currents-blog/2020/colorectal-cancer-rising-younger-adults> (accessed: March 2023).
- [3] M. Bretthauer, M. Løberg, P. Wieszczy, M. Kalager, L. Emilsson, K. Garborg, M. Rupinski, E. Dekker, M. Spaander, M. Bugajski, Ø. Holme, A. G. Zauber, N. D. Pilonis, A. Mroz, E. J. Kuipers, J. Shi, M. A. Hernán, H.-O. Adami, J. Regula, G. Hoff, M. F. Kaminski, *N. Engl. J. Med.* **2022**, *387*, 1547.
- [4] J. Pan, L. Xin, Y. F. Ma, L. H. Hu, Z. S. Li, *Am. J. Gastroenterol.* **2016**, *111*, 355.

- [9] R. Cardoso, F. Guo, T. Heisser, H. De Schutter, N. Van Damme, M. C. Nilbert, J. Christensen, A.-M. Bouvier, V. Bouvier, G. Launoy, A.-S. Woronoff, M. Cariou, M. Robaszekiewicz, P. Delafosse, F. Poncet, P. M. Walsh, C. Senore, S. Rosso, V. E. P. P. Lemmens, M. A. G. Elferink, S. Tomšič, T. Žagar, A. L. de Munain Marques, R. Marcos-Gragera, M. Puigdemont, J. Galceran, M. Carulla, A. Sánchez-Gil, M.-D. Chirlaque, M. Hoffmeister, et al., *Lancet Reg. Health – Eur.* **2022**, 21, 100458.
- [6] X. Q. Luu, K. Lee, J. K. Jun, M. Suh, K.-W. Jung, K. S. Choi, *J. Gastroenterol.* **2022**, 57, 464.
- [7] X. Li, Yi Zhou, Z. Luo, Yi Gu, Y. Chen, C. Yang, J. Wang, S. Xiao, Q. Sun, M. Qian, G. Zhao, *BMC Public Health* **2019**, 19, 1016.
- [8] M. F. Hale, R. Sidhu, M. E. McAlindon, *World J. Gastroenterol.* **2014**, 20, 7752.
- [9] P. V. Draganov, *Gastroenterol. Hepatol.* **2018**, 14, 50.
- [10] Y. Ahmed, M. Othman, *Curr. Gastroenterol. Rep.* **2022**, 22, 39.
- [11] A. G. Zauber, S. J. Winawer, M. J. O'Brien, I. Lansdorp-Vogelaar, M. van Ballegooijen, B. F. Hankey, W. Shi, J. H. Bond, M. Schapiro, J. F. Panish, E. T. Stewart, J. D. Wayne, *N. Engl. J. Med.* **2012**, 366, 687.
- [12] Y. Pang, J. Liu, Z. L. Moussa, J. E. Collins, S. McDonnell, A. M. Hayward, K. Jajoo, R. Langer, G. Traverso, *Adv. Sci.* **2019**, 6, 1901041.
- [13] Y. Saito, T. Uraoka, Y. Yamaguchi, K. Hotta, N. Sakamoto, H. Ikematsu, M. Fukuzawa, N. Kobayashi, J. Nasu, T. Michida, S. Yoshida, H. Ikehara, Y. Otake, T. Nakajima, T. Matsuda, D. Saito, *Gastrointest. Endosc.* **2010**, 72, 1217.
- [14] J. Lian, S. Chen, Y. Zhang, F. Qiu, *Gastrointest. Endosc.* **2012**, 76, 763.
- [15] A. Amato, F. Radaelli, L. Corrae, E. Di Giulio, A. Buda, V. Cennamo, L. Fuccio, M. Devani, O. Tarantino, G. Fiori, G. De Nucci, M. De Bellis, C. Hassan, A. Repic, *United Eur. Gastroenterol. J.* **2019**, 7, 1361.
- [16] S. Ito, A. Nishiguchi, F. Sasaki, H. Maeda, M. Kabayama, A. Ido, T. Taguchi, *Mater. Sci. Eng. C* **2021**, 123, 111993.
- [17] X. Hu, M. W. Grinstaff, *Gels* **2023**, 9, 282.
- [18] C. H. Park, S. K. Lee, *Clin. Endosc.* **2013**, 46, 456.
- [19] T. Iwatsubo, Y. Takeuchi, Y. Yamasaki, K. Nakagawa, M. Arai, M. Ohmori, H. Iwagami, K. Matsuno, S. Inoue, H. Nakahira, N. Matsuura, S. Shichijo, A. Maekawa, T. Kanesaka, S. Yamamoto, K. Higashino, N. Uedo, R. Ishihara, *Dig. Dis.* **2019**, 37, 53.
- [20] K. Taku, Y. Sano, K.-I. Fu, Y. Saito, T. Matsuda, T. Uraoka, T. Yoshino, Y. Yamaguchi, M. Fujita, S. Hattori, T. Ishikawa, D. Saito, T. Fujii, E. Kaneko, S. Yoshida, *J. Gastroenterol. Hepatol.* **2007**, 22, 1409.
- [21] N. G. Burgess, A. J. Metz, S. J. Williams, R. Singh, W. Tam, L. F. Hourigan, S. A. Zanati, G. J. Brown, R. Sonson, M. J. Bourke, *Clin. Gastroenterol. Hepatol.* **2014**, 12, 651.
- [22] T. Wilkins, B. Wheeler, M. Carpenter, *Am. Fam. Physician* **2020**, 101, 294.
- [23] J. Romagnuolo, *Can. J. Gastroenterol.* **2009**, 23, 158.
- [24] O. Ortiz, D. K. Rex, I. S. Grimm, M. T. Moyer, M. K. Hasan, D. Pleskow, B. J. Elmunzer, M. A. Khashab, O. Sanaei, F. H. Al-Kawas, S. R. Gordon, A. Mathew, J. M. Levenick, H. R. Aslanian, F. Antaki, D. von Renteln, S. D. Crockett, A. Rastogi, J. A. Gill, R. Law, M. B. Wallace, P. A. Elias, T. A. MacKenzie, H. Pohl, M. Pellisé, *Endoscopy* **2021**, 53, 1150.
- [25] H. Pohl, I. S. Grimm, M. T. Moyer, M. K. Hasan, D. Pleskow, B. J. Elmunzer, M. A. Khashab, O. Sanaei, F. H. Al-Kawas, S. R. Gordon, A. Mathew, J. M. Levenick, H. R. Aslanian, F. Antaki, D. von Renteln, S. D. Crockett, A. Rastogi, J. A. Gill, R. J. Law, P. A. Elias, M. Pellise, M. B. Wallace, T. A. Mackenzie, D. K. Rex, *Gastroenterology* **2019**, 157, 977.
- [26] C. Jacobs, P. V. Draganov, D. Yang, *Transl. Gastroenterol. Hepatol.* **2019**, 4, 80.
- [27] G. Muñoz Taboada, P. Dosta, E. R. Edelman, N. Artzi, *Adv. Mater.* **2022**, 34, 2203087.
- [28] S. Baghdasarian, B. Saleh, A. Baidya, H. Kim, M. Ghovvati, E. S. Sani, R. Haghniaz, S. Madhu, M. Kanelli, I. Noshadi, N. Annabi, *Mater. Today Bio* **2022**, 13, 100199.
- [29] Y. Liang, H. Xu, Z. Li, A. Zhangji, B. Guo, *Nano-Micro Lett.* **2022**, 14, 185.
- [30] C. Ghobril, M. W. Grinstaff, *Chem. Soc. Rev.* **2015**, 44, 1820.
- [31] K. Zheng, Q. Gu, D. Zhou, M. Zhou, L. Zhang, *Smart Polym. Mater. Biomed. Appl.* **2022**, 3, 41.
- [32] M. Mehdizadeh, J. Yang, *Macromol. Biosci.* **2013**, 13, 271.
- [33] A. H. C. Anthis, M. P. Abundo, A. L. Neuer, E. Tsolaki, J. Rosendorf, T. Rduch, F. H. L. Starsich, B. Weisse, V. Liska, A. A. Schlegel, M. G. Shapiro, I. K. Herrmann, *Nat. Commun.* **2022**, 13, 7311.
- [34] W. Han, B. Zhou, K. Yang, X. Xiong, S. Luan, Y. Wang, Z. Xu, P. Lei, Z. Luo, J. Gao, Y. Zhan, G. Chen, L. Liang, R. Wang, S. Li, H. Xu, *Bioact. Mater.* **2020**, 5, 768.
- [35] Y. Miura, Y. Tsuji, R. Cho, A. Fujisawa, M. Fujisawa, H. Kamata, Y. Yoshikawa, N. Yamamichi, T. Sakai, K. Koike, *Sci. Rep.* **2021**, 11, 18508.
- [36] J. He, Z. Zhang, Y. Yang, F. Ren, J. Li, S. Zhu, F. Ma, R. Wu, Yi Lv, G. He, B. Guo, D. Chu, *Nano-Micro Lett.* **2021**, 13, 80.
- [37] X. Xia, X. Xu, B. Wang, D. Zhou, W. Zhang, X. Xie, H. Lai, J. u Xue, A. Rai, Z. Li, X. Peng, P. Zhao, L. Bian, P. W.-Y. Chiu, *Adv. Funct. Mater.* **2022**, 32, 2109332.
- [38] X. Xu, X. Xia, K. Zhang, A. Rai, Z. Li, P. Zhao, K. Wei, Li Zou, B. Yang, W.-K. Wong, P. W.-Y. Chiu, L. Bian, *Sci. Transl. Med.* **2020**, 12, eaba8014.
- [39] F. H. Mourad, R. W. Leong, *J. Gastroenterol. Hepatol.* **2018**, 33, 1445.
- [40] T. Miyagi, T. Ishimine, J. Nakazato, N. Taniguchi, N. Yagi, T. Takahashi, T. Tengan, M. Wake, *JACC: Case Rep.* **2021**, 3, 53.
- [41] N. Artzi, T. Shazly, C. Crespo, A. B. Ramos, H. K. Chenault, E. R. Edelman, *Macromol. Biosci.* **2009**, 9, 754.
- [42] N. Artzi, T. Shazly, A. B. Baker, A. Bon, E. R. Edelman, *Adv. Mater.* **2009**, 21, 3399.
- [43] N. Artzi, A. Zeiger, F. Boehning, A. bon Ramos, K. Van Vliet, E. R. Edelman, *Acta Biomater.* **2011**, 7, 67.
- [44] K. Jain, P. Kesharwani, U. Gupta, N. K. Jain, *Int. J. Pharm.* **2010**, 394, 122.
- [45] R. S. Navath, A. R. Menjoge, H. Dai, R. Romero, S. Kannan, R. M. Kannan, *Mol. Pharmaceutics* **2011**, 8, 1209.
- [46] R. Das Mahapatra, K. B. C. Imani, J. Yoon, *ACS Appl. Mater. Interfaces* **2020**, 12, 40786.
- [47] P. Wang, G. Deng, L. Zhou, Z. Li, Y. Chen, *ACS Macro Lett.* **2017**, 6, 81.
- [48] R. Yan, Y. Yan, J. Gong, J. Ma, *Mater. Res. Express* **2019**, 6, 055322.
- [49] P. Ren, H. Zhang, Z. Dai, F. Ren, Y. Wu, R. Hou, Y. Zhu, J. Fu, *J. Mater. Chem. B* **2019**, 7, 5490.
- [50] H. J. Han, J. H. Jeong, J. W. Kim, W. B. Seung, *Korean J. Neurotrauma* **2020**, 16.
- [51] S.-H. Lee, C.-W. Park, S.-G. Lee, W.-K. Kim, *Korean J. Spine* **2013**, 10, 44.
- [52] H. Chen, F. Yang, R. Hu, M. Zhang, B. Ren, X. Gong, J. Ma, B. Jiang, Q. Chen, J. Zheng, *J. Mater. Chem. B* **2016**, 4, 5814.
- [53] T. Jaffe, W. M. Thompson, *Radiology* **2015**, 275, 651.
- [54] A. Kaydu, E. Gokcek, *Med. Sci. Monit.* **2018**, 24, 5542.
- [55] A. Schmassmann, A. Tarnawski, B. M. Peskar, L. Varga, B. Flogerzi, F. Halter, *Am. J. Physiol.* **1995**, 268, G276.
- [56] J. L. Roh, Y. H. Yoon, *Arch. Otolaryngol. – Head Neck Surg.* **2006**, 132, 995.
- [57] R. V. Benjaminsen, M. A. Matthebjerg, J. R. Henriksen, S. M. Moghimi, T. L. Andresen, *Mol. Ther.* **2013**, 21, 149.
- [58] H. Zhu, C. A. Hart, D. Sales, N. B. Roberts, *J. Med. Microbiol.* **2006**, 55, 1265.
- [59] E. Keskin, H. A. Aydın, M. Kalayci, E. Işık, U. Özgen, K. Şimşek, D. Baklaci, M. Gökçe, *Türk. J. Med. Sci.* **2021**, 51, 1512.
- [60] A. Kinaci, T. P. C. Van Doormaal, *Expert Rev. Med. Devices* **2019**, 16, 549.

- [61] S. Haider, M. Kahaleh, *Nat. Clin. Pract. Gastroenterol. Hepatol.* **2010**, 6, 660.
- [62] K. Fang, R. Wang, H. Zhang, L. Zhou, T. Xu, Y. Xiao, Y. Zhou, G. Gao, J. Chen, D. Liu, F. Ai, J. Fu, *ACS Appl. Mater. Interfaces* **2020**, 12, 52307.
- [63] Z. Xu, J. Li, G. Gao, Z. Wang, Y. Cong, J. Chen, J. Yin, L. Nie, J. Fu, *J. Polym. Sci., Part B: Polym. Phys.* **2018**, 56, 865.
- [64] M. C. Giano, Z. Ibrahim, S. H. Medina, K. A. Sarhane, J. M. Christensen, Y. Yamada, G. Brandacher, J. P. Schneider, *Nat. Commun.* **2014**, 5, 4095.
- [65] S. X. Jiang, D. Chahal, N. Ali-Mohamad, C. Kastrup, F. Donnellan, *Endosc. Int. Open* **2022**, 10, E1136.
- [66] B. Bang, E. Lee, J. Maeng, K. Kim, J. H.a Hwang, S.-H. Hyon, W. Hyon, D. H. Lee, *PLoS One* **2019**, 14, 0216829.
- [67] G. M. Taboada, K. Yang, M. J. N. Pereira, S. S. Liu, Y. Hu, J. M. Karp, N. Artzi, Y. Lee, *Nat. Rev. Mater.* **2020**, 5, 310.
- [68] M. Wang, P. Lu, B. Wu, J. D. Tucker, C. Cloera, Q. Lu, *J. Mater. Chem.* **2012**, 22, 6038.
- [69] ASTM F 2258-05 Standard Test Method for Strength Properties of Tissue Adhesives in Tension, **2005**, pp. 1308–1312.